6210 *J. Med. Chem.* **2010,** *53,* 6210–6227
DOI: 10.1021/jm1006534

Journal of Medicinal Chemistry Article

A New Class of Antitumor *trans*-Amine-Amidine-Pt(II) Cationic Complexes: Influence of Chemical Structure and Solvent on in Vitro and in Vivo Tumor Cell Proliferation

Cristina Marzano,[†] Silvia Mazzega Sbovata,[‡] Valentina Gandin,[†] Davide Colavito,[§] Elda Del Giudice,[§] Rino A. Michelin,[‡] Alfonso Venzo,[∥] Roberta Seraglia,[∥] Franco Benetollo,[⊥] Mariano Schiavon,[†] and Roberta Bertani*[,‡]

[†]*Department of Pharmaceutical Sciences, Universy of Padova, Via F. Marzolo 5, I-35131 Padova, Italy,* [‡]*Department of Chemical Processes of Engineering, University di Padova, Via F. Marzolo 9, I-35131 Padova, Italy,* [§]*Research&Innovation (R&I) SpA, Via Svizzera 16, I-35127 Padova, Italy,* [∥]*CNR−ISTM, Istituto di Scienze e Tecnologie Molecolari, Via F. Marzolo 1, I-35131 Padova, Italy, and* [⊥]*CNR−ICIS, Corso Stati Uniti 4, I-35127 Padova, Italy*

Received May 31, 2010

The reactions of cyclopropylamine, cyclopentylamine, and cyclohexylamine with *trans*-[$PtCl_2(NCMe)_2$] afforded the bis-cationic complexes *trans*-[$Pt(amine)_2(Z\text{-amidine})_2]^{2+}[Cl^-]_2$, **1**−**3**. The solution behavior and biological activity have been studied in different solvents (DMSO, water, polyethylene glycol (PEG 400), and polyethylene glycol dimethyl ether (PEG-DME 500)). The biological activity was strongly influenced by the cycloaliphatic amine ring size, with *trans*-[$Pt(NH_2\overline{CH(CH_2)_4CH_2})_2\{N(H){=}C(CH_3)\text{-}N(H)\overline{CH(CH_2)_4CH_2}\}_2]^{2+}[Cl^-]_2$ (**3**) being the most active compound. Complex **3** overcame both cisplatin and MDR resistance, inducing cancer cell death through p53-mediated apoptosis. Alkaline single-cell gel electrophoresis experiments indicated direct DNA damage, reasonably attributable to DNA adducts of *trans*-[$PtCl(amine)(Z\text{-amidine})_2$][Cl] species, which can evolve to produce disruptive and nonrepairable lesions on DNA, thus leading to the drug-induced programmed cancer cell death. Preliminary in vivo antitumor studies on C57BL mice bearing Lewis lung carcinoma highlighted that complex **3** promoted a significant and dose-dependent tumor growth inhibition without adverse side effects.

Introduction

In recent years, a great variety of *trans*-platinum complexes[1−6] have been shown to possess significant in vitro and in vivo antitumor activity similar to or even higher than that of *cis*-diamminedichloroplatinum(II) (cisplatin[a]), contrary to the previously described relationship between *cis*-based structure and antitumor activity of platinum drugs.[7−9] It has been proposed that one characteristic of active *trans*-$Pt(II)Cl_2L_2$ (where L = N-donor ligand) antitumor drugs is the presence, in the metal coordination sphere, of hindered ligands that can suitably reduce the rate of displacement of the chloro ligands.[10,11] Thus, monofunctional Pt-DNA adducts are formed, which can give rise to interstrand and/or protein interactions that are responsible for the drug-induced cytotoxic effect.[12] This has been explored with Pt(II) complexes of the type *trans*-[$PtCl_2LL'$], where L and L′ are pyridine-like ligands,[13,14] alkyl-substituted amines,[15,16] iminoethers,[17−19] or the recently described phosphines[20] and acetoximes[21] and Pt(IV) complexes with *trans*-[$PtCl_2X_2LL'$] configuration where X is a hydroxide or carboxylate ligand and L and L′ are amines.[22−28] The biological activity of dinuclear dicationic platinum complexes of the type *trans*-[$\{Pt(NH_3)_2Cl\}\mu$-dpzm]$^{2+}$, where dpzm is 4,4′-dipyrazolylmethane,[29] and [$\{Pt(Me)Cl(Me_2SO)\}_2(\mu\text{−N-N})$], where N−N is $H_2N(CH_2)_6NH_2$,[30,31] has been investigated. Recently, a new class of polynuclear Pt(II) complexes, which can be described as two *trans*-[$PtCl(NH_3)_2$] units that are linked by bridging *trans*-[$Pt(NH_3)_2\{H_2N(CH_2)_6NH_2\}_2$] tetra-amines, has been proposed. This class of complexes entered phase I clinical trials with the lead compound BBR3464.[32] It is noteworthy that only a few cationic platinum complexes have been screened and have demonstrated in vitro and in vivo antitumor activity.[33] Recently, the DNA binding of platinum complexes containing cationic, bicyclic, nonpolar piperidinopiperidine (pip-pip) ligands has been demonstrated.[34]

Recent results have shown that *trans*-complexes exhibit cytotoxic activity because of their general ability to overcome cisplatin resistance owing to their distinct cellular pharmacological properties with respect to cisplatin, which are caused

*To whom correspondence should be addressed. Phone: +39-49-827-5731. Fax: +39-49-827-5525. E-mail: roberta.bertani@unipd.it.

[a] Abbreviations: Cisplatin, *cis*-diamminedichloroplatinum(II); MTT, 3-(4,5-dimethylthiazol-2-yl)-2,5-diphenyltetrazolium bromide; DMSO, dimethyl sulfoxide; PEG400, polyethylene glycol 400; PEGDME500, poly (ethylene glycol) dimethyl ether; DMF, dimethylformamide; MDR, multidrug resistance; PBS, phosphate buffered saline; HMG, high mobility group proteins; NMR, nuclear magnetic resonance; GC/MS, gas chromatography/mass spectrometry; ESI-MS, electrospray ionization mass spectrometry; COSY, correlation spectroscopy; TOCSY, total correlation spectroscopy; NOESY, nuclear Overhauser enhancement spectroscopy; EXSY, exchange spectroscopy; HMQC, heteronuclear multiple quantum correlation; HMBC, heteronuclear multiple bond correlation; HEPES, *N*′-2-hydroxyethylpiperazine-*N*′-2 ethanesulphonic acid; LLC, Lewis lung carcinoma; DTT, 1,4-dithiothreitol; AFC, 7-amino-4-trifluoromethylcoumarin; SYBR green, 2-[*N*-(3-dimethylaminopropyl)-*N*-propylamino]-4-[2,3-dihydro-3-methyl-(benzo-1,3-thiazol-2-yl)-methyli-dene]-1-phenyl-quinolinium; SDS, sodium dodecyl sulfate; IC_{50}, half maximal inhibitory concentration; FACS, flow cytometry; RT-PCR, reverse transcriptase polymerase chain reaction.

 Published on Web 08/03/2010

Scheme 1. Synthesis of Bis-amidine Pt(II) Complexes

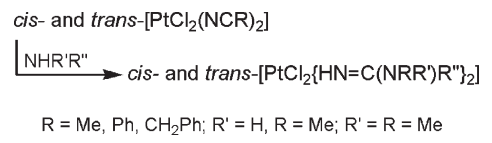

by the differing interactions of the compounds with DNA.[5,35−38] *trans*-Platinum compounds form interstrand cross-links, which stabilize the DNA double helix, whereas cisplatin forms an intrastrand cross-link pattern.[3,13]

We have recently been investigating the biological activity of a series of Pt(II) bis-amidine complexes[39,40] with the general formulas *cis*- and *trans*-$[PtCl_2\{N(H)=C(NHMe)R\}_2]$ and *cis*- and *trans*-$[PtCl_2\{N(H)=C(NMe_2)R\}_2]$ (where R = Me, Ph, CH_2Ph), which are obtained by the nucleophilic addition of primary and secondary aliphatic amines to *cis*- and *trans*-di(nitrile) Pt(II) complexes (Scheme 1).

Similar to the iminoether ligands in the *cis*-$[PtCl_2\{N(H)=C(OMe)CH_2Ph\}_2]$[41] and *trans*-$[PtCl_2\{N(H)=C(OR)Me\}_2]$ (R = Me, Et)[17−19] derivatives, amidines maintain the presence of the imino moiety NH=C(sp^2) bonded to the platinum center. Furthermore, amidines derived from primary amines bear an additional NH group, which is known to be responsible for important hydrogen-bond donor properties when approaching the biological target[42] and can interact with DNA to potentially form new types of lesions. Amidines are also versatile ligands because their lipophilicity can be tuned by modification of the R group.

The introduction of cyclic aliphatic amines, in particular cyclohexylamine, in the platinum coordination sphere, may be of interest because of their steric hindrance and flexibility, resembling nonplanar heterocyclic amine ligands such as 4-picoline, piperidine, or piperazine.[43−49] The cyclohexylamine ligand has been reported in a new class of potential anticancer drugs of the type *trans*-[(NHC)PtI_2(amine)], which are characterized by the presence of N-heterocyclic carbenes (NHC) in the metal coordination sphere.[49]

The presence of the cyclohexyl ring[28,50,51] also characterizes the series of platinum complexes that are based on the 1,2-diaminocyclohexane (DACH) carrier ligand. Two of these compounds, Oxaliplatin and Ormaplatin, have entered clinical trials.[22,52,53]

The first orally active platinum complex that is active against several human ovarian carcinoma xenografts was *trans*,*trans*,*trans*-$[PtCl_2(OH)_2(NH_3)$(cyclohexylamine)] (JM335);[22] however, it was found to be significantly less active than cisplatin because of its inactivation by cellular thiols.[54−57]

Cyclohexylamine is present as a spectator ligand in *cis*,*trans*,*cis*-$[PtCl_2(NH_3)(C_6H_{11}NH_2)(OCOCH_3)_2]$ (JM216, Satraplatin), which was reported to be highly active in vitro against both Pt-sensitive and Pt-resistant human tumor cell lines.[44,58] The influence of cyclohexylamine as a spectator ligand in *cis*-$[PtCl_2(NH_3)(C_6H_{11}NH_2)]$ (JM118), one of the two major metabolites of JM216, was thoroughly examined. It was observed that domain A of HMGB1 was the most sensitive to the nature of the spectator ligands on platinum and that the affinity that HMG box proteins have for Pt-modified DNA depends on the base pairs immediately flanking the platinum adduct.[44] The X-ray structure of the asymmetric complex $[Pt(NH_3)$(cyclohexylamine)$]^{2+}$ bound to a dodecamer DNA duplex was also reported.[59] The bulky cyclohexylamine increases the hydrophobicity of the major groove in the vicinity of the adduct, thereby affecting drug activity, along with hydrogen bonding and other major groove interactions between the protein, DNA, and the ligands on the platinum center. One of these compounds, Satraplatin, in combination with prednisone, has been submitted for approval by the FDA for the treatment of hormone-refractory prostate cancer.[60] Recently, another of these compounds $[Pt(NH_3)$(cyclohexylamine)$(OOC\text{-}CH_2\text{-}COO)]$ was reported to provide greater DNA platination and cytotoxic activity against human leukemia HL60 and human bladder carcinoma EJ cells than cisplatin.[51]

Furthermore, the biological activities of *trans*-$[PtCl_2$(dimethylamine)(cyclohexylamine)] and *trans*-$[PtCl_2(OH)_2$(dimethylamine)(cyclohexylamine)] were also reported, and it was shown that these compounds are active against a panel of tumor cell lines in the low micromolar range and exhibit the same significant antitumor activity against cell lines that are either sensitive to or have acquired resistance to cisplatin.[26] After treatment with these compounds, only a small percentage of cancer cells underwent apoptosis, with most of the cellular population dying through a necrosis-like mechanism. It was also shown that these platinum complexes induced a complete blockade at the S phase of the cell cycle, inhibiting total mRNA transcription and precluding p53 activation.[61]

From this perspective, we report the synthesis, characterization, and biological activity of a new class of cationic *trans*-Pt(II) complexes of the type *trans*-$[Pt(amine)_2(amidine)_2][Cl]_2$ that are derived from the reaction of *trans*-$[PtCl_2(NCCH_3)_2]$ with cyclopropylamine, cyclopentylamine, and cyclohexylamine. These complexes are characterized by the following features: (i) the presence of four N-ligands bonded to the platinum center, which resemble the antitumor drugs that are prepared by the reaction of transplatin with oligonucleotides containing a GNG triplet (where N is any nucleoside),[5] (ii) the presence of two aliphatic amine ligands in a *trans* position, which can undergo exchange processes, (iii) the presence of two amidine ligands, which bear the planar N(H)=C moiety, similar to the iminoether systems,[17−19] as carrier ligands, (iv) the amidine ligands in a *Z* configuration, which are more biologically active than the *E* configuration in iminoether complexes,[62] and (v) solubility in both organic solvents and water.

The cytotoxic properties of the new derivatives have been assessed using a large panel of human cancer cell lines that belong to a variety of different tumor types and include cisplatin- and multidrug-resistant (MDR) phenotypes. Their cytotoxicity against normal human fibroblasts was also tested. Specific attention was focused on the effect induced by the ring size of the amine ligands (cyclopropylamine, cyclopentylamine, or cyclohexylamine) and by the solvent used to carry out the biological assays. We have investigated and compared the solution behavior by dissolving the new compounds in solvents such as DMSO, water, polyethylene glycol (PEG 400), and polyethylene glycol dimethyl ether (PEG-DME 500), with the aim of overcoming solubility and toxicity problems. The putative mechanism(s) of cytotoxicity for this new class of *trans*-Pt compounds was investigated by cellular pharmacology studies in 2008 human ovarian adenocarcinoma cells. In particular, DNA damage, apoptosis and p53 induction, and cell cycle perturbations were monitored and compared to those caused by cisplatin. Finally, a preliminary in vivo evaluation of the anticancer activity of *trans*-$[Pt(NH_2\overline{CH(CH_2)_4CH_2})_2\text{-}\{N(H)=C(CH_3)N(H)\overline{CH(CH_2)_4CH_2}\}_2]^{2+}[Cl^-]_2$ (compound **3**), which was selected as the lead compound, was performed in the Lewis lung carcinoma (LLC) tumor model.

Scheme 2. Synthesis of Compounds **1**−**3**

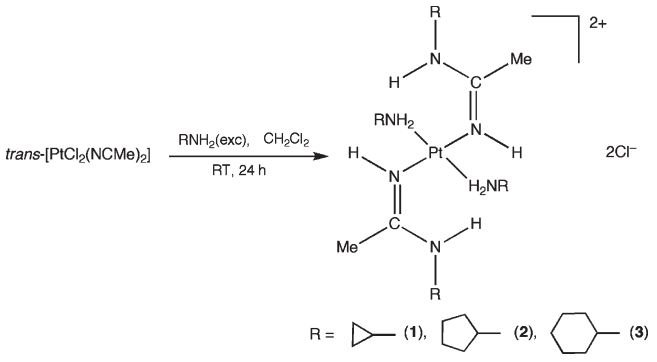

Results and Discussion

Chemistry. Synthesis and Characterization of the Complexes. The reaction of excess cycloaliphatic amine, RNH_2 (R = cyclopropyl-, cyclopentyl-, or cyclohexyl-) with *trans*-$[PtCl_2(NCMe)_2]$, carried out in CH_2Cl_2 at room temperature for 24 h, provided the dicationic *trans*-$[Pt(amine)_2(Z\text{-amidine})_2]^{2+}[Cl^-]_2$, **1**−**3** complexes in high yield (approximately 80%) (Scheme 2). The amidine ligands **1**−**3** are formed by nucleophilic addition of the cyclic aliphatic amine to the nitrile triple bond as previously reported for similar reactions.[39,40] Further reaction of RNH_2 at the platinum center caused displacement of the coordinated chlorides.

It should be noted that the same reactions performed at low temperature (−20 °C) and for short reaction times (5 h) produced a mixture of neutral and cationic bis-amidine complexes, *trans*-$[PtCl_2(Z\text{-amidine})_2]$, and *trans*-$[PtCl(amine)_2(Z\text{-amidine})_2]^+[Cl^-]$, respectively.[63]

Chloride substitution by an entering amine was previously described for the reaction of K_2PtCl_4 and *trans*-$[PtCl_2(NCMe)_2]$ with ammonia[64−67] or aliphatic diamines[68] and was also reported in the reaction of *trans*-$[PtCl_2(NCMe)_2]$ with isopropylamine.[69] The absorption of excess of gaseous ammonia by CH_2Cl_2 solutions of *cis*- and *trans*-$[PtCl_2(NCR)_2]$ (R = NMe_2, NEt_2, NC_5H_{10}, Et, CH_2Ph, or Ph) was recently reported to yield *cis*- and *trans*-$[(NH_3)_2\{NH{=}C(NH_2)R\}_2][Cl]_2$[70] compounds.

The infrared spectra of complexes **1**−**3** were characterized by the presence of the C=N absorption at about 1620 cm^{-1} and a band at about 420 cm^{-1} that is attributed to the Pt−N vibration, in agreement with data reported in the literature for complexes of the type $[Pt(cycloalkylamine)_2X_2]$ (X = Cl, I).[71,72] The coordination of the corresponding amine to the platinum center was confirmed by the presence in the ^1H NMR spectra of N−H signals at about 5 ppm flanked by ^{195}Pt satellites with coupling constants of approximately 50 Hz. It is noteworthy that in cyclic aliphatic amine complexes, the two protons on each carbon atom are not equivalent; the proton on the same side of the N atom is more deshielded than the other, giving rise to a second-order proton NMR spectrum. It is known that the strength of the Pt−N σ bond can be related to the basicity of the ligand.[72] The formation of the σ bond between the amine N and Pt should transfer some electron density from the amine to the Pt atom, resulting in a shielding of the metal center and a deshielding effect on the ligands (^1H and ^{13}C signals). The presence of two amidines as ancillary ligands would increase the electron density of the metal compared to the amine complexes $[Pt(cycloalkylamine)_2I_2]$. These mechanisms are in agreement with the ^{195}Pt chemical shift (δ) that was observed at −3487 ppm for compound **2**; the resonance was more shielded compared to the δ value of −3350 ppm that was found for the $[Pt(cycloalkylamine)_2I_2]$ complexes.[72,73] The signals of the NH_2 protons were significantly deshielded with respect to the data that were reported for the *trans*-$[Pt(cycloalkylamine)_2I_2]$ complexes, which is in agreement with the higher deshielding effect due to the presence of donor ancillary ligands, such as amidines, compared to iodines. We found no correlation between the ^{13}C, ^1H, and Pt−H coupling constant values of complexes **1**−**3** and the published proton affinity of the amines, with pK_a values of 8.67, 9.98, and 9.85 for cyclopropylamine, cyclopentylamine, and cyclohexylamine, respectively.[72] The ^{15}N NMR spectrum of compound **2** showed the presence of three N signals at δ values of −256.4 ($^1J_{NH}$ = 90 Hz, HNC_5H_9), −270.1 ($^1J_{NH}$ = 80 Hz, PtNH), and −376.3 ppm of the platinum-coordinated NH_2 moiety. This latter signal exhibited the lowest N−H coupling constant value ($^1J_{NH}$ = 70 Hz), confirming the existence of the expected sp^3 nitrogen hybridization.[74,75] The chemical shift of the N atom of the coordinated cyclopentylamines of compound **2** (δ = −376.3) resulted in an upfield shift compared to that of the free amine (δ = −338.4), which is in agreement with data reported in the literature for primary aliphatic amines and the corresponding hydrochlorides.[76] The amidine ligands in compounds **1**−**3** were magnetically equivalent, giving rise to a unique set of signals in the ^1H NMR spectra. The *Z* configuration was confirmed by NOESY experiments, which showed a correlation between the signals of the Pt−NH and the CH_3 protons.

The fragmentation pathways of compounds **1**−**3** dissolved in CH_3CN under ESI conditions involved the formation of ionic species corresponding to $[Pt(AD)_2(AM)_2]^{2+}$, $[PtCl(AD)_2(AM)_2]^+$, $[Pt(AD)_2(AM)_2\text{-}H]^+$, and $[PtCl(AD)_2(AM)]^+$ (AD = amidine ligand, AM = amine ligand), as confirmed by MS/MS experiments and isotope pattern analysis.

X-ray Crystal Structure of Compound 1. Summaries of the refinement results and other crystallographic information are provided in the Supporting Information. The ORTEP diagram for compound **1** is shown in Figure 1 with selected bond distances and angles. The complex was crystallized in the triclinic system, and the coordination at the Pt metal center was *trans* planar. The square planar coordination geometry around the Pt atom was characterized by Pt−N(2) and Pt−N(2)′ bond distances of 2.006(4) Å, which is in agreement with the literature[39,64,66,77,78] for similar amidine Pt(II) complexes. The amidine ligands were shown to be in the *Z* configuration. The N(2)−C(4) and N(3)−C(4) bond distances were 1.297(6) and 1.341(7) Å, respectively, suggesting the presence of an electronic delocalization along the N−C−N system. The C−N bond distances were in the range that has been observed for *trans*-bis-amidine complexes such as *trans*-$[Pt(Pr^iNH_2)_2\{Z\text{-}N(H){=}C(NHPr^i)Me\}_2][Cl_2]$ (values between 1.25(1) and 1.37(1) Å),[78] *trans*-$[PtCl_2\{Z\text{-}N(H){=}C(NHBu^t)Me\}_2]$ (values between 1.304(4) and 1.321(5) Å),[77] and *trans*-$[PtCl_2\{Z\text{-}N(H){=}C(NHMe)CH_2Ph\}_2]$ (values between 1.278(8) and 1.324(9) Å).[78] The N(2)−Pt(1)−N(2)′ (180°), N(1)−Pt(1)−N(1)′ (180°), and N(1)−Pt−N(2), N(1)−Pt−N(2)′ (87.7(2)° and 92.3(2)°) angles showed the expected values for a square planar coordination geometry around the Pt atom.[79,80] In the cyclopropylamine ligands, the Pt−N distance (2.055(4) Å) was comparable to values reported in *cis*-$[PtCl_2(C_3H_5NH_2)_2]$[81] and *cis*-$[Pt(C_3H_5NH_2)_2(C_6H_7N_2O_2)_2]\cdot 2H_2O$[82] complexes. It is noteworthy that the Pt−N(amidine) distance was shorter (2.006(4) Å) than that of Pt−N(amine) (2.055(4) Å), which indicates a greater stability

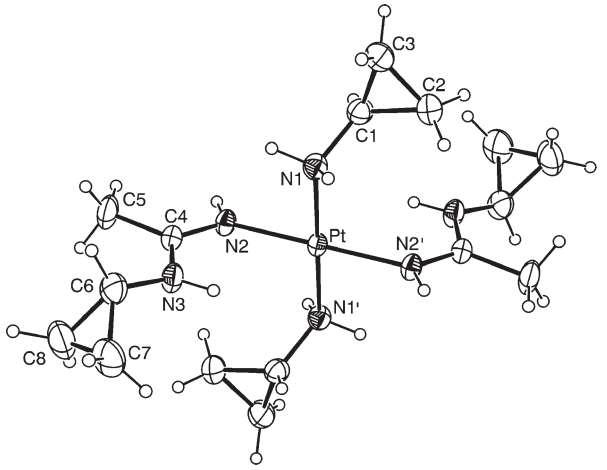

Figure 1. ORTEP diagram for *trans*-[Pt(NH$_2$CHCH$_2$CH$_2$)$_2${N(H)=C(CH$_3$)N(H)CHCH$_2$CH$_2$}$_2$]$^{2+}$ cation. Displacement ellipsoid are drawn at the 40% probability. Selected averaged bond distances (Å): Pt−N(1), 2.055(4); Pt−N(2), 2.006(4); N(1)−C(1), 1.458(7); N(2)−C(4), 1.297(6); N(3)−C(4), 1.341(7); N(3)−C-(6),1.434(7). Angles (deg): N(1)−Pt−N(2), 87.7(2); N(1)−Pt−N(2)′, 92.3(2); C(1)−N(1)−Pt,114.5(3); C(4)−N(3)−C(6); 123.7(5); C(4)−N(2)−Pt, 127.1(3); N(2)−C(4)−N(3), 120.3(4).

of the coordinated amidines compared to the coordinated amines in the ligand displacement processes. This value was in agreement with what was reported for one of the two crystalline forms of *trans*-[Pt(Pr^{i}NH$_2$)$_2${*Z*-N(H)=C(NHPr^i)-Me}$_2$][Cl$_2$],[68] with a Pt−N(amidine) distance of 1.988(7) Å. The other one had an Pt−N(amidine) bond distance of 2.035(8) Å, which is comparable to the reported values of Pt−N bonds in [Pt(NH=SPh$_2$)$_2${NH=C(Me)N=SPh$_2$}$_2$]-[PF$_6$][83] and *trans*-[PtCl$_4${N(H)=C(Et)(NHC$_5$H$_4$N)}$_2$].[84]

Solution Behavior. To improve the solubility,[85] the biological activity of the amidine complexes **1**−**3** was investigated by dissolving them in DMSO, water, PEG 400 (average molecular weight = 380−420), and PEG-DME (average molecular weight = 500).

a. DMSO. It is known that the simultaneous administration of cisplatin and DMSO significantly reduces the nephrotoxicity of the drug.[86] Moreover, the previously observed[86−89] antitumor activity of cationic platinum species bearing coordinating sulfoxides seems to be based on the properties of DMSO, which shows a large *trans*-effect and a fairly weak *trans*-influence as a coordinating ligand.[90] It was previously reported that even after a long period of time (48 h) at room temperature in DMSO, *trans*-[PtCl$_2$(NH$_3$)$_2$] formed only *trans*-[PtCl(NH$_3$)$_2$(DMSO)][Cl].[91,92] The substitution of a coordinated chlorine was also observed by dissolving the bis-amidine derivatives, *trans*-[PtCl(NH$_3$){HN=C(NH$_2$)R}$_2$][Cl] (R = Me, Ph, CH$_2$Ph) in DMSO, which resulted in the formation of *trans*-[Pt(DMSO)(NH$_3$){HN=C(NH$_2$)R}$_2$][Cl]$_2$.[39] The behavior of the cationic compounds **1**−**3** after solubilization in DMSO was studied using NMR and ESI-MS. A unique species was formed by dissolving compound **2** in DMSO-d_6 containing 0.5% DMSO-h_6 for 24 h as indicated by a singlet at a δ value of −3356 in the ^{195}Pt NMR spectrum, which was assigned to the monocationic amine-diamidine species, [PtCl(NH$_2$CH(CH$_2$)$_3$CH$_2$){N(H)=C(CH$_3$)N(H)CH(CH$_2$)$_3$CH$_2$}$_2$]$^+$[Cl$^-$], based on the NMR and ESI data. The ^{1}H NMR spectrum showed signals at δ values of 4.83 ($^1J_{PtH}$ = 66 Hz, NH$_2$), 5.87 (PtNH), and 8.05 (d, $^3J_{HH}$ = 6 Hz, NH) in the ratio 1:1:1, highfield shifted with respect to the corresponding resonances of the starting compound **2**. The displacement in compound **2** of cyclopentylamine by DMSO was confirmed by GC/MS analysis of the NMR solution, which showed the presence of a free cyclopentylamine peak (m/z = 85, retention time = 8.25 min). Similar results were observed by dissolving compounds **1** and **3** in DMSO-d_6. With GC/MS, it was observed that the process was completed in 15 min. Monitoring of the reaction of compound **2** with 5 equiv of DMSO-h_6 in CDCl$_3$ using ^{1}H NMR, a singlet at a δ value of 3.37 was observed. The corresponding ^{13}C nucleus resonated at a δ value of 51.92. These signals could be attributed to the methyl groups of coordinated DMSO slowly exchanging with the free DMSO, as indicated by EXSY experiments in an intermediate species.

The ESI fragmentation pattern of compound **2** in DMSO is reported in Scheme 3. The base peak is represented by ions with an m/z of 567, which corresponds to the monocationic species, [PtCl{NH$_2$CH(CH$_2$)$_3$CH$_2$}{N(H)=C(CH$_3$)N(H)-CH(CH$_2$)$_3$CH$_2$}$_2$]$^+$. Five coordinated ionic species at m/z values of 652 and 347.5, which were formed by addition of Cl$^-$ and DMSO, respectively, were also observed.

b. Water. The ^{1}H NMR spectrum of compound **2** in D$_2$O showed the disappearance of the NH signals due to fast H−D exchange processes, together with the appearance of a new signal at a δ value of 3.90, which is attributable to the CH proton of the free cyclopentyl amine, the formation of which was confirmed by GC/MS analysis of the NMR solution. After dissolving compound **2** in acetone-d_6 and then adding two equivalents of H$_2$O, complex ligand substitution processes occurred, as demonstrated by the appearance in the ^{1}H NMR spectrum of the resonances of four different amidine ligands in an approximate 2:2:1:2 ratio, (PtNH signals at δ values of 6.89, 6.67, 6.41, and 6.18; NH signals at δ values of 8.56, 7.68, 7.77, and 7.37), together with a broad resonance at a δ value of 4.91 ($^1J_{PtH}$ = 63 Hz). A very small signal at a δ value of 4.80 could be assigned to metal-coordinated water on the basis of NOESY experiments. The detection of free cyclopentylamine by GC/MS in the NMR solution again indicated amine displacement. The ESI MS spectrum of compound **2** in water showed the presence of the ionic species, [PtCl{NH$_2$CH(CH$_2$)$_3$CH$_2$}{N(H)=C(CH$_3$)N(H)CH(CH$_2$)$_3$CH$_2$}$_2$]$^+$ as the base peak at an m/z of 567 (Scheme 3).

c. PEG. PEG is widely used in drug delivery[93,94] and has been studied as a modifying agent that is able to improve the solubility of drugs; in particular, it has been tested with some platinum systems.[95−97] On this basis, we also dissolved the amidine complexes **1**−**3** in low molecular weight liquid PEGs to explore their use as solvents in the cytotoxicity tests. We used either PEG 400 (PEG-OH) or PEG-DME (PEG-OMe), the latter of which was specifically considered to prevent the occurrence of possible reductive processes that might be induced by the OH moieties of PEG-OH. The stability of complexes **1**−**3** in PEG 400 was studied by ^{1}H NMR upon dissolution of the compounds in CDCl$_3$ with an excess of glycol. The NMR spectrum of complex **2** shows the presence of two sets of resonances, indicating the presence of two species in an approximately 2:1 ratio. The most abundant

Scheme 3. ESI MS Fragmentation Pathways of Compounds **1**−**3** in Different Solvents

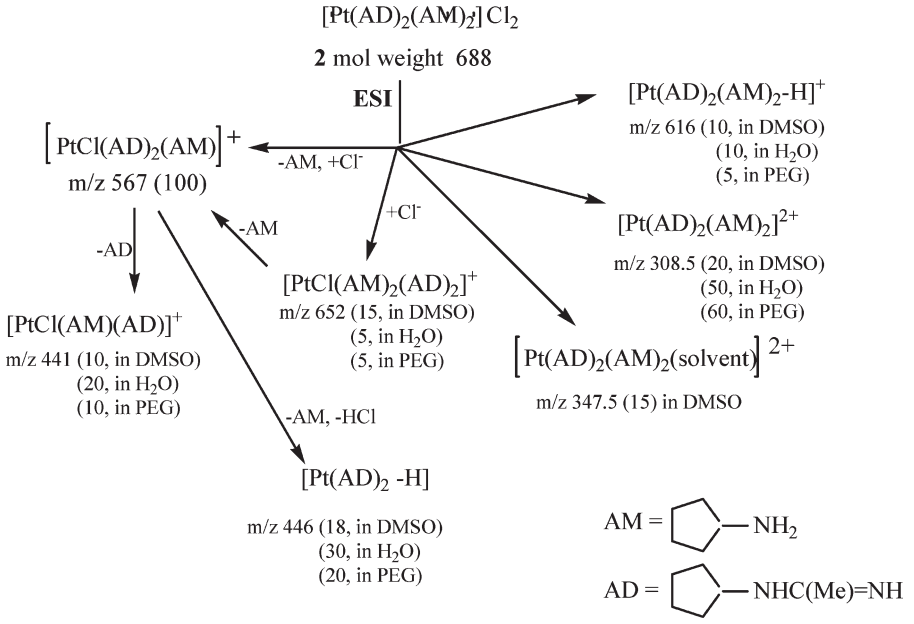

species gave rise to signals in the NH region at δ values of 8.68, 6.88, and 4.80 in the integral ratio of 1:1:2, which are attributed to the C=NH, Pt-NH, and C_5H_9-NH_2 protons, respectively, of compound **2**. The second species was characterized by a new set of signals at δ values of 7.54, 7.13, and 5.98 with an integral ratio of 1:1:1, which could probably be assigned to the monocationic species, $[PtCl(NH_2\overline{CH(CH_2)_3CH_2})\{N(H)=C(CH_3)N(H)\overline{CH(CH_2)_3CH_2}\}_2]^+[Cl^-]$. The interaction of PEG 400 with the metal center was also suggested by the presence in the ^1H NMR spectrum of two broad signals at δ values of 3.2 and 3.0, which were assigned to the OH protons of coordinated and free glycol, respectively, and were shown by NOESY experiments to be involved in an exchange process. The amine displacement process was confirmed by GC/MS analyses, which showed the presence of free amine in the NMR solution. The ESI MS spectrum of the NMR solution showed the presence, as the base peak (Scheme 3), of the ionic species, $[PtCl(NH_2\overline{CH(CH_2)_3CH_2})\{N(H)=C(CH_3)N(H)\overline{CH(CH_2)_3CH_2}\}_2]^+$, at an m/z of 567. Similar experiments have been carried out in which the amidine complexes were dissolved in PEG-DME 500. Despite the fact that the solubilities of the amidine complexes in this solvent were lower, it was observed that derivatives **1**−**3** caused amine displacement, as confirmed by GC/MS analysis.

Biology. Cytotoxicity Tests. The dicationic *trans*-bis-amidine Pt(II) derivatives **1**−**3** were evaluated for their cytotoxic properties against a panel of human tumor cell lines, which contained examples of cervix (HeLa), breast (MCF-7), lung (A549), and colon (HCT-15) cancer, and melanoma (A375). Moreover, Pt(II)-amidine complexes were tested for their cytotoxicity against normal human fibroblasts (HFF-1). For comparison, the cytotoxicity of transplatin and cisplatin were examined.

We investigated and compared the antiproliferative activity of compounds **1**−**3** by dissolving them in water, DMSO, PEG 400, or PEG-DME 500. The IC_{50} values, calculated from the dose−survival curves, obtained after 48 h of drug treatment in the MTT test, are summarized in Figure 2.

Despite the fact that compounds **1**−**3** showed appreciable water solubility, their aqueous solutions proved to be totally ineffective when they were tested for cytotoxic activity by the MTT test (data not shown). This lack of biological activity can be tentatively attributed to the very low lipophilicity of compounds **1**−**3**, as indicated by the values of octanol−water partition coefficient (Kow) of compounds **1**−**3** being much less than 1, most likely reducing their ability to cross the plasmalemma. Moreover, we suggest the occurrence of equilibria which involve ligand exchange and give rise to species that have too low of a lipophilicity and consequently an unsuitable kinetic stability with respect to the ligand displacement reactions.

In Figure 2A, the results that were obtained by dissolving complexes **1**−**3** in DMSO are reported. Complex **1** showed a detectable cytotoxic activity that was markedly lower than that of the reference drug, cisplatin, with average IC_{50} values over five cell types that were about 3 times higher than those of cisplatin (mean IC_{50} values (μM) of 76.62 and 27.6 for compound **1** and cisplatin, respectively). In contrast, derivatives **2** and **3** showed significant in vitro antitumor activity. In particular, complex **3** distinguished itself as the most promising derivative, eliciting a growth inhibitory potency that was markedly higher than that of cisplatin. In HeLa cervix carcinoma cells, the cytotoxicity of compound **3** exceeded that of the reference drug by a factor of about 1.5 and in both HCT-15 colon and MCF-7 breast carcinoma cells by a factor of about 4. Noticeably, against A549 lung cancer cells, which are barely chemosensitive to cisplatin,[98] the cytotoxicity of complex **3** exceeded that of the reference metallodrug by a factor of about 5, confirming its ability to overcome intrinsic cisplatin resistance. The cytotoxic activity of derivative **2** appeared to be relevant but lower (about 1.2-fold) than that of the reference drug, with mean IC_{50} values of 36.07 and 29.56 μM for compound **2** and cisplatin, respectively. Nevertheless, all of the dicationic *trans*-bis-amidine complexes appeared to be more effective than transplatin, which has been well documented[1−6] to be scarcely effective toward all cancer cell lines.

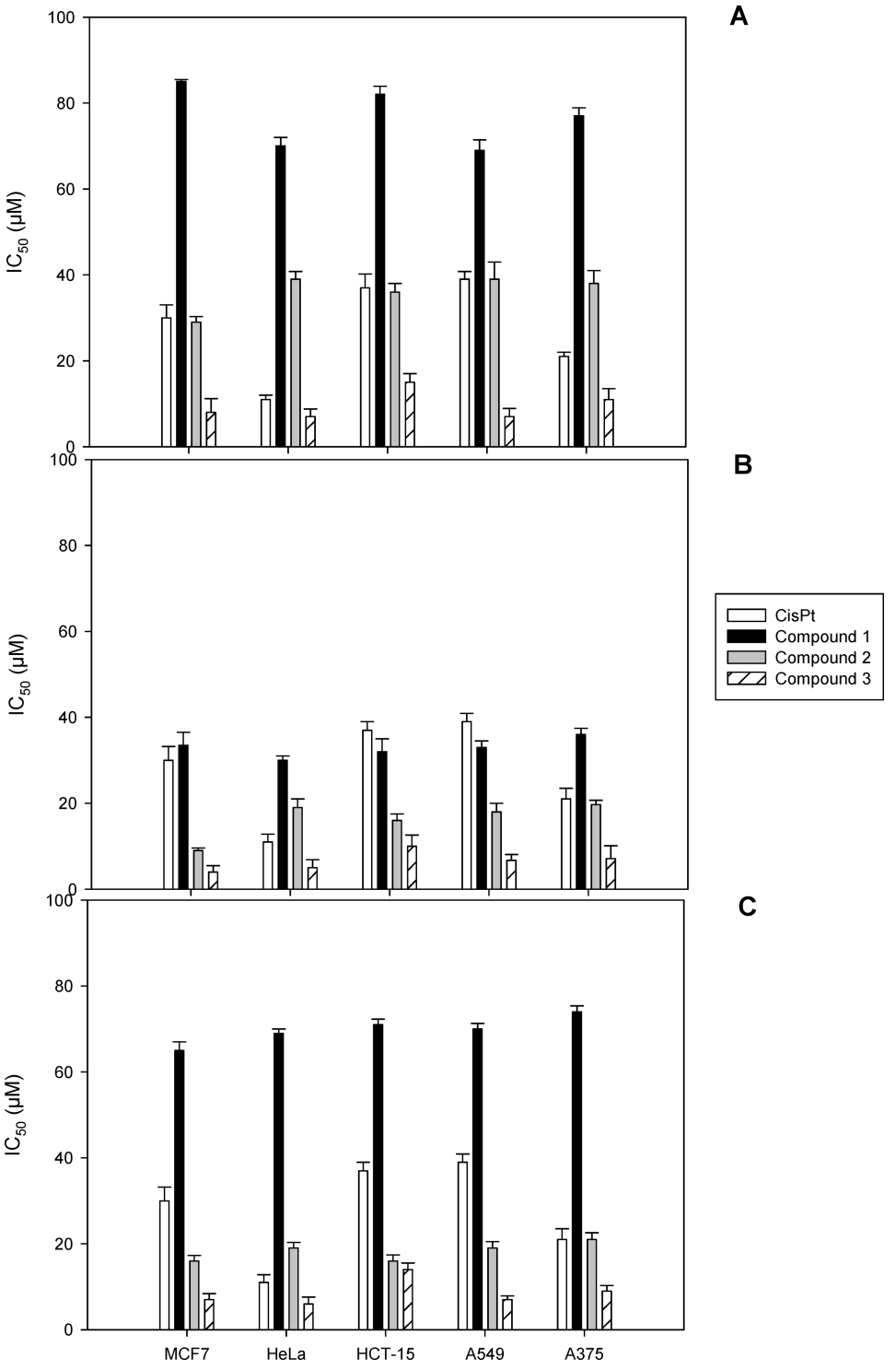

Figure 2. In vitro antitumor activity. Cells ($3-8 \times 10^3 \cdot mL^{-1}$) were treated for 48 h with increasing concentrations of the tested compounds. Cytotoxicity was assessed by the MTT test. The IC_{50} values were calculated by probit analysis ($P < 0.05$, χ^2 test). Values are shown as mean (±standard deviation (SD)) of three independent experiments. (A) Complexes dissolved in DMSO. (B) Complexes dissolved in PEG 400. (C) Complexes dissolved in PEG-DME 500. Cisplatin was dissolved in water.

Rather different observations have to be made about the growth inhibitory activity displayed by the bis-amidine derivatives that were dissolved in PEG 400 and PEG-DME 500. As shown in Figure 2B, by dissolving derivatives **1**−**3** in PEG 400, we have detected, for all tested compounds, a significant increase in the in vitro antitumor activity. Complex **1** was characterized by a cytotoxicity similar to that exhibited by cisplatin, whereas compound **2** appeared to be much more active, exhibiting average IC_{50} values that were approximately 2-fold lower than those of cisplatin (mean IC_{50} (μM) values of 16.3 and 27.6 for compound **2** and cisplatin, respectively). Compound **3** was the most effective bis-amidine Pt(II) derivative. In fact, the in vitro antitumor activity of derivative **3** was in the low micromolar range toward all tumor cell lines, exceeding that of the reference drug by a factor ranging from approximately 2.5 to 8, with

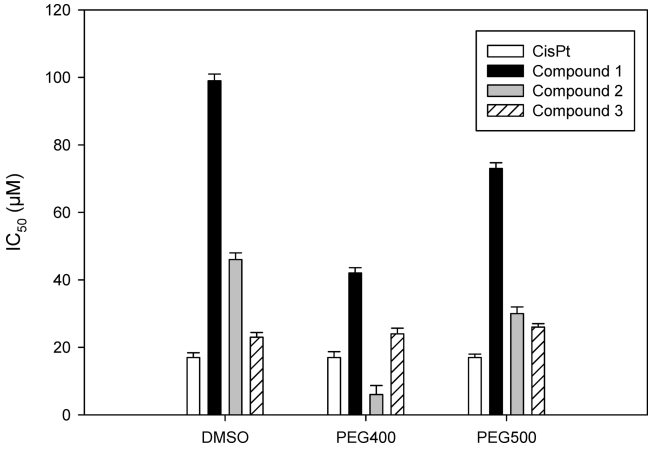

Figure 3. Cytotoxicity against nontumor cells. Cells ($5 \times 10^4 \cdot mL^{-1}$) were treated for 48 h with increasing concentrations of the tested compounds. The cytotoxicity was assessed by the MTT test. The IC_{50} values were calculated by probit analysis ($P < 0.05$, χ^2 test). Cisplatin was dissolved in water. The values are shown as the mean (±SD) of three independent experiments.

mean IC_{50} values and ranges of 6.4 μM (4.0−10.0) and 27.6 μM (11.0−39.1) for compound **3** and cisplatin, respectively. Finally, in Figure 2C, the IC_{50} values obtained by solubilizing derivatives **1**−**3** in PEG-DME 500 are reported. All of the compounds maintained a pattern of response across the various cell lines that was similar to that obtained in PEG 400, although a slight decrease in cytotoxic potency was recorded for all of the derivatives, most likely due to a lower solubility in this solvent.

Interestingly, as shown in Figure 3, HFF-1 human normal fibroblasts seemed to be less affected than tumor cells by treatment with the Pt(II) amidine complexes. Complexes **1**−**3**, dissolved in all three solvents, appeared to be at least 1.5-fold less cytotoxic toward nontumor cells than cisplatin was, indicating a potential selectivity of these compounds for cancer cells.

The encouraging results that were obtained against the in-house panel of cancer cell lines prompted us to study the cytotoxic activity of compounds **1**−**3** on additional human cancer cell lines, including cisplatin-resistant cells (C13* ovarian adenocarcinoma cells, which were suitably selected in vitro after a continuous treatment with increasing cisplatin concentrations), cisplatin-revertant cells (RH4 ovarian adenocarcinoma cells, a cisplatin-sensitive cell line that was obtained from C13* after reverting the cisplatin resistance), and two MDR phenotypes (LoVo/MDR colon adenocarcinoma cells and A2780ADR ovarian adenocarcinoma cells, which were suitably selected in vitro for their resistance to doxorubicin). On the basis of the observations previously mentioned, we chose PEG 400 as the most appropriate solvent for these investigations. The in vitro antitumor activity was assessed after a 48 h exposure, with the MTT test (Figure 4). The cross-resistance profiles were evaluated by means of the resistance factor (RF), which is defined as the ratio between the IC_{50} values calculated for the resistant cells and the sensitive ones.

In C13* ovarian carcinoma cells, cisplatin resistance is correlated to reduced cellular drug uptake,[99] enhanced repair of DNA damage,[100] and high cellular levels of glutathione and thioredoxin reductases.[101] As shown in Figure 4, derivatives **1**−**3** demonstrated a similar cytotoxic potency both on cisplatin-sensitive and -resistant cell lines. The RF calculated for all compounds was about 6- to 9-fold lower than that of cisplatin, clearly indicating that there were no cross-resistance phenomena. RH4 revertant cells were obtained from C13* cells by selection with the lipophilic cation, Rh123. The RH4 cells lost a substantial portion of their cisplatin resistance, being only 2- to 3-fold resistant to cisplatin. Despite this major loss of resistance, they retained a number of the phenotypic features that are related to cisplatin resistance and which were observed in C13* cells.[102] Complexes **1**−**3**, when tested in RH4 cisplatin-revertant cells, showed cytotoxic activity that was similar to that observed in 2008 and C13* cells.

Acquired MDR, whereby cells become refractory to multiple drugs, poses an important challenge to the success of anticancer chemotherapy. The resistance of colon cancer LoVo/MDR and ovarian cancer A2780ADR cells to doxorubicin, a drug belonging to the MDR spectrum, is associated with overexpression of different species of multispecific drug transporters.[103,104] Despite the fact that cisplatin is not a P-glycoprotein substrate, MDR protein 2 (MRP2) is able to transport the platinum complex and is responsible for its efflux from the cell.[105]

Cytotoxicity assays that tested the amidine derivatives **1**−**3** against these MDR cancer cell line pairs showed a similar pattern of response across the parental and the resistant sublines. In particular, RF values calculated for all derivatives were about 23 to 30 times lower than those recorded with doxorubicin, suggesting that compounds **1**−**3** are not potential MDR substrates.

DNA Damage and p53 Involvement in Apoptosis Induction. The cytotoxicity data highlighted the fact that compound **3** dissolved in PEG400 was the most powerful derivative of the compounds tested in this work. Therefore, it was used in additional cellular pharmacology studies. The experiments were performed in 2008 human ovarian carcinoma cells, and the results were compared to cisplatin, the first-line chemotherapeutic drug against ovarian cancer.

It has been reported that cisplatin, which targets DNA, induces cell death in cancer cells by triggering an extrinsic apoptosis pathway through the activation of the caspase cascade.[106] Moreover, one of the early effects of the cisplatin-induced platination of DNA is a reduction in the rate of DNA synthesis and a consequent dose-dependent arrest in the S phase.[107]

To characterize the cell death pathway that was triggered by derivative **3**, we examined its effects in terms of induction of apoptosis and cell cycle modifications.

Because caspase-3 is a well-known executor enzyme in the apoptosis pathway, we investigated the ability of compound **3** to activate caspase-3 in 2008 human ovarian cancer cells. As shown in Figure 5, treatment with IC_{50} concentrations of compound **3** resulted in a significant enhancement of enzyme activity. In particular, the protease activity was enhanced by factors of about 5 and 1.2 in cells that were treated for 24 h with derivative **3** over untreated and cisplatin-treated cells, respectively.

With the aim of investigating the cellular effects that are induced by complex **3** in terms of cell cycle modifications and induction of apoptosis, a time-dependent evaluation of the cell cycle profile was performed by FACS in 2008 cancer cells treated with IC_{50} concentrations of derivative **3**. As reported in Table 1, the percentage of 2008 ovarian cancer cells in different cell cycle phases was markedly modified by treatment for 24 h with compound **3**. In particular, exposure to complex **3** caused a 13-fold increase in the percentage of cells

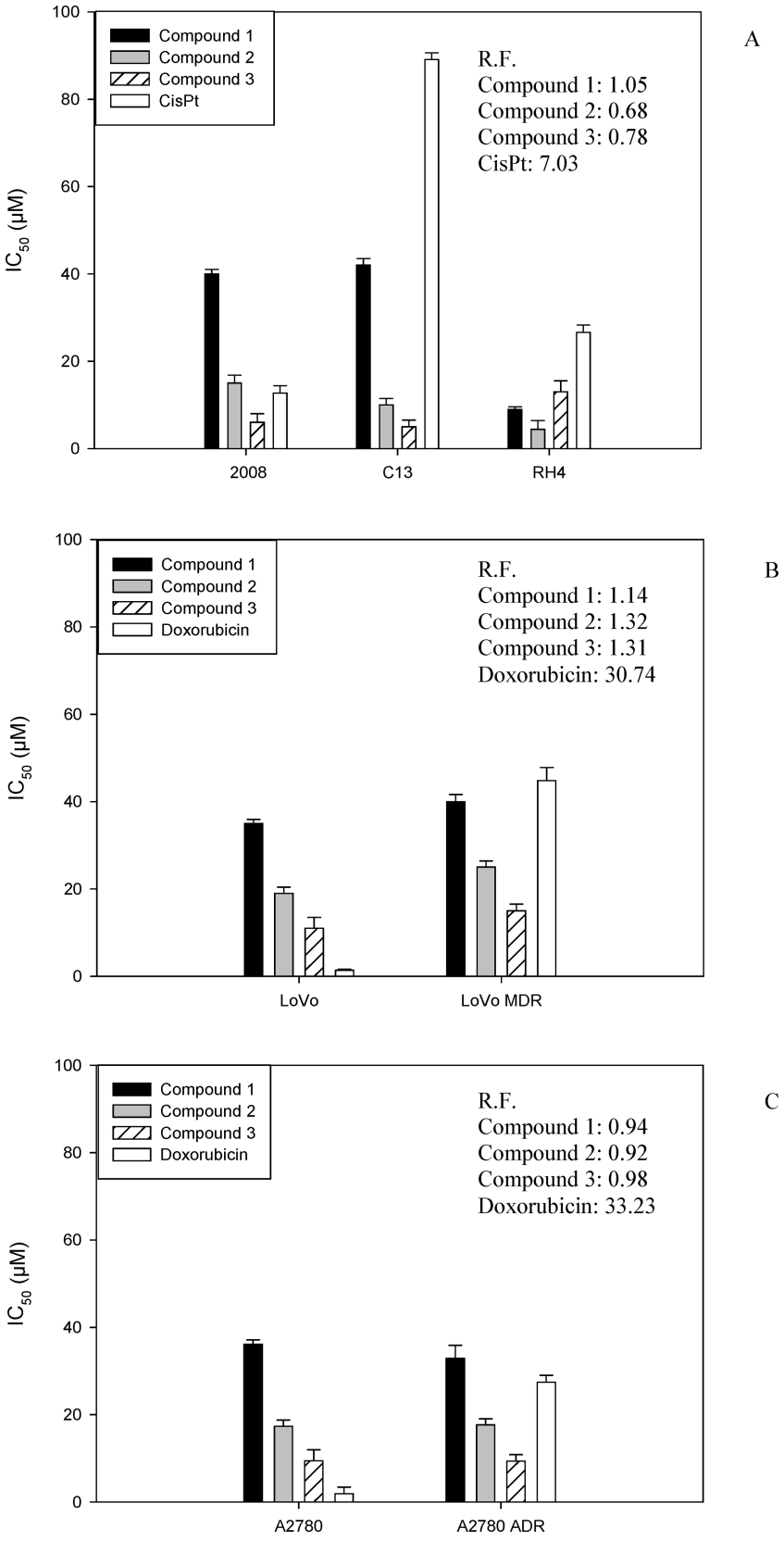

Figure 4. Cross-resistance profiles. Cells ($3-5 \times 10^3 \cdot mL^{-1}$) were treated for 48 h with increasing concentrations of the tested compounds dissolved in PEG 400. Cisplatin and doxorubicin were dissolved in water. The IC_{50} values were calculated by probit analysis ($P < 0.05$, χ^2 test). The cytotoxicity was assessed by the MTT test. The values are shown as the mean (±SD) of three independent experiments. The RF is defined as IC_{50} resistant/parent line.

with hypodiploid DNA (sub-G1 phase cells), which is considered a marker of apoptotic cell death compared to the control sample.[108,109] Apoptosis induction is likely to be related to DNA damage by platinum drugs, and one hallmark

of the DNA damage-response pathway is the induction of tumor suppressor p53, which plays a pro-apoptotic role by inducing and downregulating cell death effectors. Moreover, p53 is one of the major mediators of cisplatin-induced DNA damage,[110] and it has been previously demonstrated that the cisplatin apoptotic pathway is strictly related to p53 cascade activation.[110]

To investigate whether the complex **3**-induced apoptotic response is dependent on the transactivation of p53, we performed cytofluorimetric experiments (Table 1) by pretreating 2008 cells with pifithrin-α (PFTα) (30 μM for 12 h), a small molecule that reversibly and selectively blocks p53-dependent transcriptional activation and apoptosis.[111] For comparison, the same experiment was performed with the reference chemotherapeutic drug, cisplatin.

These cytofluorimetric experiments showed that PTFα efficiently affected the apoptotic response of cells treated with cisplatin or *trans*-bis-amidine derivative **3**, markedly decreasing the percentage of cells in the sub-G1 phase, which was provoked by the platinum compounds. In particular, pretreatment for 12 h with 30 μM of PFTα lowered the compound **3**- and cisplatin-induced sub-G1 peak by about 80% with respect to the control cells. These results suggest that the p53-associated pathway may largely contribute to complex **3**-induced apoptosis in 2008 human ovarian cells.

It has been shown that an increased expression of p53, in response to treatment with a variety of DNA-damaging agents, leads cells to cell cycle arrest and apoptotic cell death.[112] In particular, cisplatin treatment has been previously demonstrated to markedly increase both protein and mRNA p53 levels as a downstream molecular determinant, leading to apoptosis induction. The ability of compound **3** to induce p53 mRNA was analyzed by means of semiquantitative RT-PCR analysis (Figure 6A). Treatment of 2008 cells with an IC_{50} concentration of *trans*-bis-amidine **3** for 24 h resulted in significant up-regulation of p53 mRNA levels. In particular, p53 gene expression in compound **3**-treated cells was 1.4 times higher than in control cells, similar to that caused by cisplatin. Furthermore, by means of Western blot analysis, the amount of p53 protein was estimated to have increased by 3 times in complex **3**-treated cells compared to control cells (Figure 6B). These results demonstrate that complex **3** induced the expression of the p53 tumor suppressor protein as a response to cytotoxic stress, in a similar manner as cisplatin, indicating that p53 may play a key role in the apoptotic death induced by compound **3**.

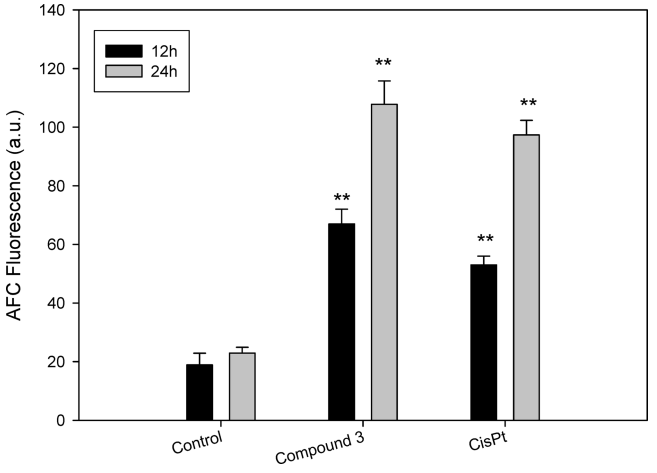

Figure 5. Induction of caspase-3 activity: 2008 cells were incubated for 12 and 24 h with compound **3** or cisplatin and then processed for caspase-3 activity detection as described in the Experimental Section. Data are the means of at least three independent experiments. Error bars indicate SD $^{**}P < 0.001$ compared to untreated cells.

The p53 response is most likely related to different types of DNA interaction. Recently, some *trans*-platinum planar amine complexes were shown to promote a marked p53 induction that was consistent with the promotion of DNA strand breaks and interstrand cross-links, which are characteristic features of *trans*-platinum complexes.[12] Therefore, we have also investigated the ability of complex **3** to induce DNA damage, compared to cisplatin, by performing alkaline single-cell gel electrophoresis (comet assay). This assay allows detection of DNA strand breaks, alkaline-labile DNA sites, and cross-links in individual cells. When a cell possessing damaged or fragmented DNA is subjected to electrophoresis and then stained with an intercalating agent, it appears as a comet, and the length and fluorescence intensity of the comet tail represents the extent of the DNA damage. The 2008 cells were treated with IC_{50} values of compound **3** and cisplatin (Figure 7A) for different incubation times (6−48 h) or exposed to an increasing concentration of the tested compounds for 24 h (Figure 7B) and monitored for comet tail appearance by fluorescence microscopy. Compared to control 2008 cells, both compound **3**- or cisplatin-treated cells displayed a dose- and time-dependent increase in electrophoretic migration of the DNA fragments, evidenced by the outline resembling comet formation. This behavior has been confirmed by the calculation of two different parameters, the tail length (Figure 7, a, and 7B, b) and the tail moment (Figure 7A, a′, and 7B, b′), which were calculated from the captured images with CellF software. The tail length (length of DNA migration), which is directly related to the DNA fragment size, was calculated from the center of the cell and measured in micrometers. The tail moment was calculated as the product of the tail length and the fraction of DNA in the comet tail. In Figure 7C, representative images of 2008 control (a) and comet-positive cells that were treated for 12 h (b) are displayed.

Although the comet assay is mainly used to identify DNA strand breaks, it has recently been modified to study the induction of DNA cross-linking.[113] Therefore, the treatment of 2008 cells with the tested platinum complexes was followed by exposure with H_2O_2 (1 μM) for 30 min to induce DNA strand breaks. As reported in Figure 7D,E, different exposure times with an IC_{50} concentration of compound **3** and cisplatin induced a significant reduction of comet tail

Table 1. Cell Cycle Profiles[a]

phase	control	cisplatin	cisplatin + PFTα	compd **3**	**3** + PFTα	PFTα
sub-G1	1.9 ± 0.9	24.7 ± 1.5	4.19 ± 0.7	26.1 ± 1.0	5.2 ± 0.6	2.4 ± 0.3
G1	62.6 ± 1.2	44.2 ± 1.8	68.8 ± 1.2	41.4 ± 1.3	79.1 ± 0.2	59.2 ± 1.1
S/G2/M	36.1 ± 2.2	29.8 ± 1.9	26.9 ± 0.8	31.3 ± 1.7	17.7 ± 1.1	38.4 ± 0.9

[a] Percentage of cells in different cell cycle phases after 24 h exposure with IC_{50} concentrations of compound **3** and cisplatin with or without PFTα vs control untreated cells.

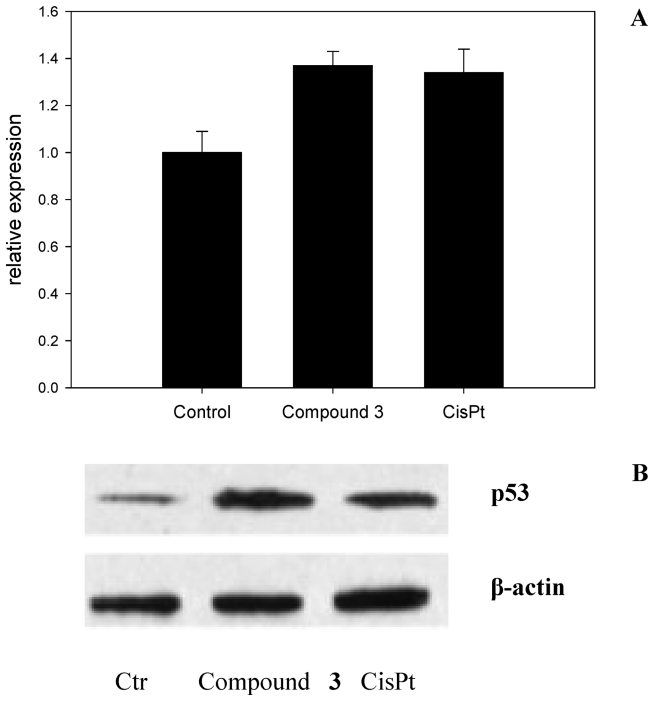

Figure 6. Induction of p53 expression (A) and activity (B). (A) 2008 cells were treated for 24 h with an IC_{50} concentration of compound **3** or cisplatin. The relative expression of p53 mRNA was measured with RT-PCR. Results are expressed as relative amounts compared to untreated cells. The expression values for each RT-PCR product were normalized to their respective β-actin expression. The bars denote the standard error of the mean. (B) 2008 cells were treated with IC_{50} concentrations of compound **3** and cisplatin for 24 h. The amount of p53 was detected by Western blotting analysis as described in the Experimental Section.

length compared to the H_2O_2-treated control cells. This was an expected effect of cisplatin. In fact, cisplatin-induced DNA cross-links, which decrease the DNA electrophoretic mobility, had been previously documented in a modified comet assay.[114] A similar effect was observed following treatment with complex **3**, which markedly decreased the cancer cell nucleoid tail, suggesting that compound **3** has the ability to induce DNA cross-links.

In Vivo Studies. Acute Toxicity. The acute toxicity of complex **3** was assessed over 30 days by treating BALB/c mice with a single ip injection of different amounts (2.5/5/10/20/50/100 mg/kg) of the tested compounds. The animals were observed for 24 h for signs of toxicity and mortality. The result, expressed as the median lethal dose (LD_{50}) of 35 mg/kg, indicated that complex **3** has a lower acute toxicity than cisplatin (LD_{50} = 11.4 mg/kg).

Anticancer Activity toward LLC Solid Murine Tumor. To confirm the antitumor activity of compound **3**, the LLC tumor model was used in inbred C57BL mice. Tumor growth inhibition induced by complex **3** was compared with that promoted by the reference metallodrug, cisplatin. At 3, 5, 7, 9, 11, and 13 days after tumor inoculation, mice bearing tumor cells received three doses (3, 6, or 12 mg/kg, corresponding to about one-tenth, one-sixth, and one-third of the LD_{50}, respectively) of compound **3** or 1.5 mg/kg, corresponding to about one-tenth of the LD_{50}, of cisplatin. Tumor growth was estimated at day 15, and the results are summarized in Table 2. For assessment of the potential adverse effects, we measured the body weight of the animals every two days (Figure 8). Amidine derivative **3** exerted a statistically significant antitumor activity ($P < 0.05$), compared to vehicle-treated mice, even at the lower daily dose of 3 mg/kg (tumor growth inhibition of 43.72%). Remarkably, a mean 68% reduction in tumor volume occurred following treatment with 12 mg/kg of compound **3**, denoting an anticancer activity comparable to that of cisplatin (72.60%). Hence, treatment with amidine complex **3** decreased tumor weight at necropsy in a dose-dependent manner, without inducing any adverse effects including significant body weight loss throughout the therapeutic experiment in the treated groups (Figure 8). Mice treated with amidine derivative **3** showed no anorexia, whereas those treated with the reference platinum-based drug appeared prostrate and showed substantial weight loss.

Conclusions

When tested for their cytotoxicity upon dissolution in DMSO, the dicationic bis-amidine *trans*-Pt(II) complexes **1**−**3** showed significant in vitro antitumor activity. In particular, a reasonable relationship between structure and bioactivity has emerged; by increasing the alicyclic ring size, an enhancement of cytotoxic potency was achieved. Complex **3**, bearing the cyclohexyl ring, proved to be the most powerful derivative of the three. Compounds **1**−**3** displayed an appreciable increase in activity when dissolved in PEG 400 or PEG DME 500, which was about 2- to 3- times higher than their activity in DMSO, again confirming that the most active derivative is the complex bearing the cyclohexylic ring, in agreement with a general feature reported in the literature. The difference in biological activity between compounds **1**−**3** that was observed when they were dissolved in PEG and PEG-DME can be related to a masking effect due to the PEG chain on the structure of the compounds. The slight decrease of the cytotoxic effects of compounds **1**−**3** dissolved in PEG-DME 500 compared to those obtained by dissolving the compounds in PEG 400 is probably due to a general lower solubility in the former solvent.

In conclusion, the data reported here indicate that PEG 400 and PEG-DME 500 can be used as suitable solvents for platinum compounds that are frequently insoluble and/or unstable in water, DMSO, and DMF. Considering that the effects of PEG 400 and PEG-DME 500 are not identical, it can be suggested that they might be chosen to tune the solubility of the platinum complexes that are under examination. Furthermore, when PEG 400 was used as a solvent for the amidine platinum complexes, compound **3**, besides being efficiently cytotoxic against cancer cells in vitro, showed a notable anticancer effect in vivo. Because the anticancer activity in vivo also depends on various factors such as biological stability, pharmacokinetics, drug exposure pattern, drug penetration into tumor tissue, and retention time in the cancer tissue, our results confirm the appropriateness of using PEG 400 as a platinum solvent in preclinical studies.

As a final consideration for the kind of compounds tested in this paper, the most intriguing and promising results have been obtained with the dicationic complex, *trans*-$[Pt(NH_2\overline{CH(CH_2)_4CH_2})_2\{N(H)=C(CH_3)N(H)\text{-}\overline{CH(CH_2)_4CH_2}\}_2]^{2+}[Cl^-]_2^-$ (**3**). It is noteworthy that although cationic complexes of the type $[Pt(DMSO)(diam)]^{2+}$ (diam = bidentate amine) have been shown in the past to be substantially inactive in vivo, "due perhaps to the bis-positive charge and to the inability to enter the cell",[87] charged

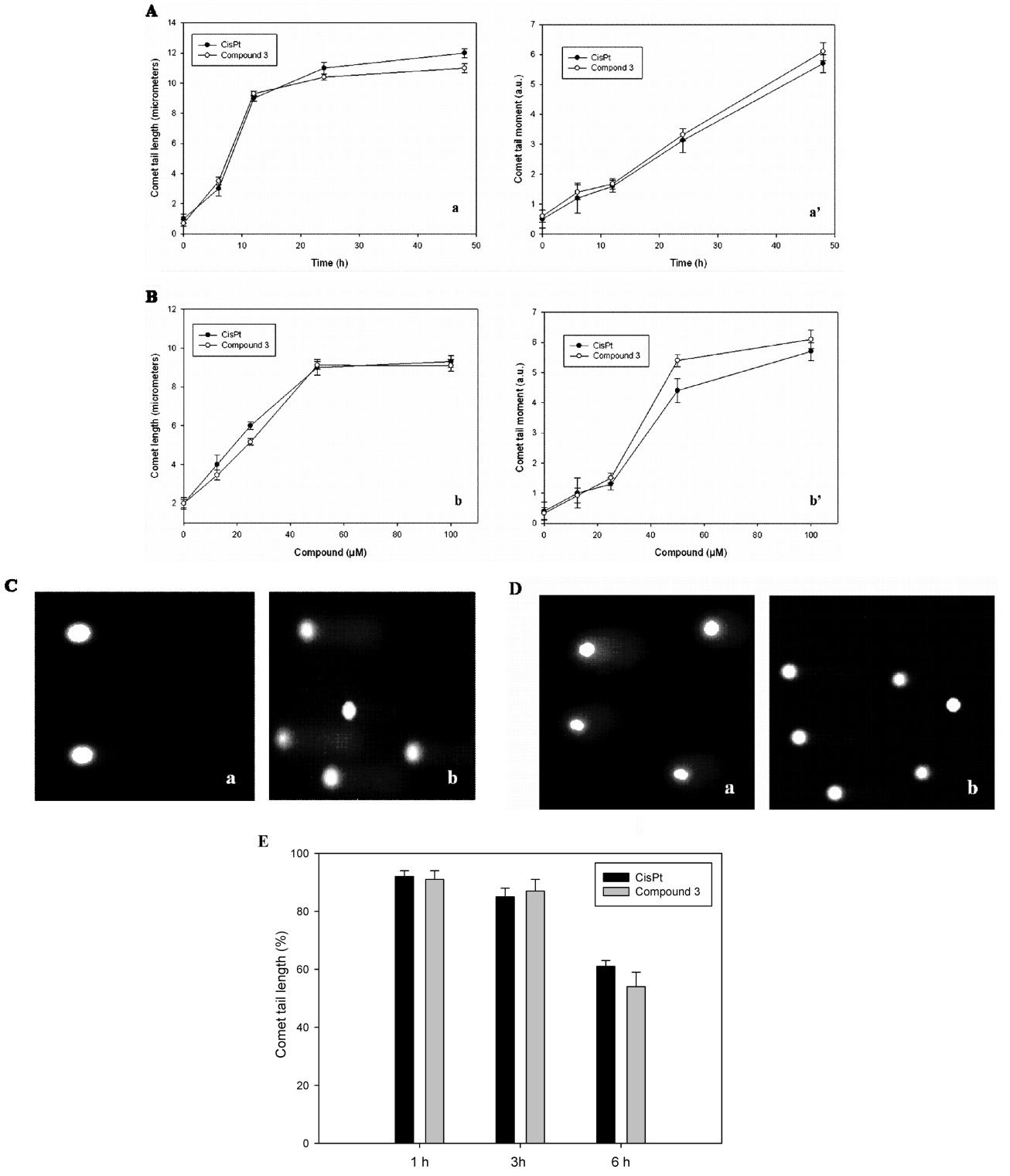

Figure 7. Single-cell gel electrophoresis data in 2008 cells (comet assay). Induction of DNA damage (A,B,C: no H_2O_2 treatment). 2008 cells treated for different incubation times (6−48 h) with IC_{50} values of compound **3** and cisplatin (A) or treated with increasing concentrations of the tested compounds for 24 h (B). The dose- and time-dependent effect of compound **3** and cisplatin treatment was evaluated by detecting the increase of comet tail length (a and b) and comet tail moment (a′ and b′). The data are the means of three independent experiments. The error bars indicate the SD. (C) Representative images of 2008 cells after 12 h incubation: (a) control and (b) IC_{50} compound **3**-treated cells. DNA cross-linking (D,E). (D) Representative images of 2008 control (a) and IC_{50} compound **3**-treated (b) cells after 3 h of exposure. (E) Comet tail length of 2008 cells treated with an IC_{50} concentration of complex **3** or cisplatin for different exposure times and subsequently with H_2O_2 (1 μM) for 30 min. The data are the means of three independent experiments. The error bars indicate the SD.

complexes where two *trans*-$[PtCl_2(NH_3)_2]$ units are linked by a tetra-amine bridge, *trans*-$[Pt(NH_3)_2\{H_2N(CH_2)_6NH_2\}_2]$, (BBR3464), have entered phase I clinical trials.[32] The tetra-amine skeleton resembles that of compounds **1**−**3**; therefore the biological activity of cationic compounds **1**−**3** may derive from the increased solubility in the cell culture medium,

Table 2. In Vivo Anticancer Activity toward Murine Lewis Lung Carcinoma (LLC)[a]

compd	daily dose ($mg \cdot kg^{1-}$)	average tumor weight (mean ± SD, g)	inhibition of tumor growth (%)
control		0.613 ± 0.05	
3	3	0.345 ± 0.11	43.72
3	6	0.278 ± 0.08	54.65
3	12	0.198 ± 0.02	67.70
cisplatin	1.5	0.168 ± 0.10	72.60

[a] Day 1: tumor implantation. Days 3, 5, 7, 9, 11, and 13: ip administration of the tested compounds. Day 15: mice sacrificed and tumors explanted.

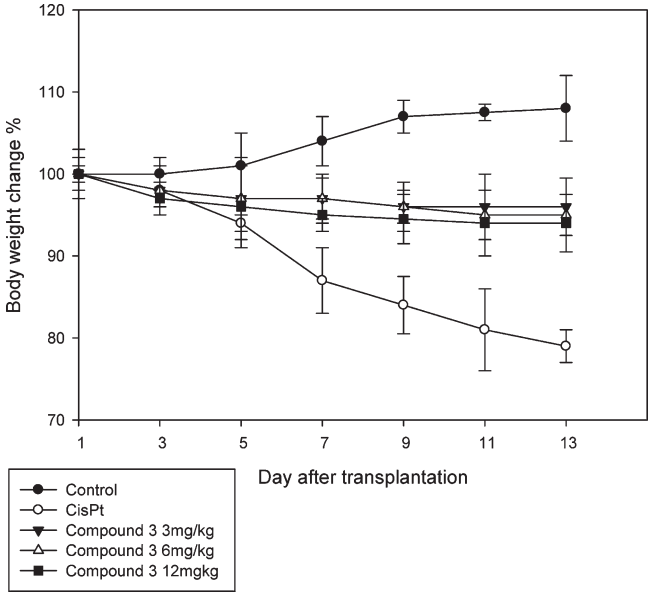

Figure 8. Body weight changes during in vivo studies. The body weight changes of LLC-bearing C57BL mice treated with vehicle or tested compounds. Each drug was administered five times at 2-day intervals, and the weights were simultaneously detected. The error bars indicate the SD.

electrostatic and H-bonding interactions with DNA, or from the occurrence of ligand exchanges. Complex **3** represents an example of a new class of complexes which deserves more thorough study; they are known to form easily when *trans*-$[PtCl_2(NCR)_2]$ reacts with amines at room temperature for a long time, preventing the presence of isomers or byproduct and giving rise to pure compounds that are suitable for biological assays. The high biological activity might be due to the formation within the cell of a unique species of the type *trans*-$[PtCl(amine)(amidine)_2][Cl]$, which originates by chloride coordination in the presence of a high concentration of Cl^- on a preliminarily formed platinum species that bears a coordinating solvent as a labile ligand. Complex **3**, distinguishing itself as the most representative dicationic bis-amidine *trans*-Pt(II) complex, was able to overcome both cisplatin and MDR resistance, inducing cell death through p53-mediated apoptosis. Direct DNA damage, reasonably attributable to DNA adducts of the *trans*-$[PtCl(amine)(amidine)_2][Cl]$ species, which can evolve to produce disruptive and nonrepairable lesions on DNA, may underlie a mechanistic explanation of drug-induced programmed cancer cell death. Finally, from the interesting results gained with in vivo testing, complex **3** emerged as a lead compound for the improvement of therapeutic potential of *trans*-platinum drugs. Interestingly, complex **3** has shown an anticancer effect against the aggressive preclinical LCC tumor model that was roughly equivalent to that obtained by using the parent drug cisplatin without inducing adverse systemic effects.

Experimental Section

General Methods. Reagents and solvents were obtained from commercial sources and used as supplied. The infrared spectra were taken on a Perkin-Elmer Spectrum 100 FT IR Spectrophotometer (CsI films); the wavenumbers ($\bar{\nu}$) are given in cm^{-1}. ^1H, ^{13}C, and ^{15}N NMR solution spectra were obtained at 298 K (unless otherwise stated) on a Bruker Avance-400 spectrometer (9.4 T field) operating at 400.13, 100.61, and 40.56 MHz, respectively, and using a Bruker 200 AC spectrometer operating at 200.12 and 50.32 MHz for ^1H and ^{13}C, respectively; δ values (parts per million, ppm) are relative to Me_4Si for ^1H and ^{13}C and relative to CH_3NO_2 for ^{15}N. Suitable integral values for the proton spectra were obtained with a prescan delay of 10 s. The assignments of the proton resonances were performed by standard chemical shift correlations, as well as by COSY, TOCSY, and NOESY experiments. In the phase-sensitive NOESY measurements the presence of intense cross-peaks, in phase with the diagonal, indicates a chemical exchange between the correlated nuclei (EXSY).[115,116] The ^{13}C resonances were attributed through 2D-heterocorrelated COSY experiments: heteronuclear multiple quantum correlation (HMQC) with bilinear rotation decoupling[117] and quadrature along F1 achieved using the time proportional phase increment method[118] for the hydrogen-bonded carbon atoms, heteronuclear multiple bond correlation (HMBC)[119,120] for the quaternary ones. The ^{15}N resonances were attributed through gradient-powered HMQC and HMBC experiments optimized on direct[117,118] and long-range[119,120] NH coupling constants, respectively. ^{195}Pt NMR spectra were recorded on a Bruker Avance 300 BB at 64.395 MHz; aqueous K_2PtCl_4 (−1628 ppm in D_2O) was the external standard. The purity of compounds **1**−**3** was stated to be higher than 95% by elemental analyses which were performed by the Microanalysis Laboratory of the Department of Chemical Sciences, University of Padova. ESI-MS analyses were performed using a Finningan LCQ-Duo ion-trap instrument, operating in positive ion mode (sheathgas flow N_2 30 au, source voltage 4.0 kV, capillary voltage 21 V, capillary temperature 200 °C). The He pressure inside the trap was kept constant. The pressure directly read by an ion gauge (in the absence of the N_2 stream) was 1.33×10^{-5} Torr. The collision-induced dissociation experiments were performed by applying a supplementary RF voltage (tickle voltage) to the end-caps of the ion trap in the range 0−80% of its maximum value (5 V peak to peak). Sample solutions were prepared by dissolving the compounds (1 mg) in the solvents as indicated in the text. The NMR solutions of the compounds were diluted 10000 times with acetonitrile to carry out ESI-MS analyses. Sample solutions were introduced into the ESI source by a syringe pump at 8 μL/min flow rate. All mass spectra were recorded on freshly prepared solutions. GC/MS analyses have been carried out with a QMD1000 instrument: column PS264 30mt; He 1 mL/min; from 100 to 280 °C, 10 °C/min. All work was carried out under a N_2 atmosphere using standard Schlenck techniques. All solvents were reagent grade and were distilled prior to use. Deuterated solvents were purchased from Cambridge Isotope Laboratories (CIL) and stored under nitrogen atmosphere.

Syntheses. *Trans*-$[PtCl_2(NCMe)_2]$ was synthesized as described in the literature.[121,122]

Complexes **1**−**3** have been prepared by a similar procedure described in detail for **1**.

trans-$[Pt(NH_2\overline{CHCH_2CH_2})_2\{N(H)=C(CH_3)N(H)\overline{CHCH_2CH_2}\}_2]^{2+}[Cl^-]_2$ (**1**) A suspension of *trans*-$[PtCl_2(NCMe)_2]$ (300 mg, 0.86 mmol) in CH_2Cl_2 (30 mL) was treated with a 5-fold excess of

cyclopropylamine (300 μL, 4.3 mmol; ρ = 0.824 g/mL). The reaction mixture was stirred at room temperature for 24 h, and then the volume was concentrated to ca. 10 mL under reduced pressure. *N*-Hexane (40 mL) was added and the suspension was stirred for 1 h. The precipitate was then filtered off at room temperature and washed with Et_2O (3 × 15 mL). Yield 367 mg, 74%. IR: ν_{N-H} 3439, 3227, 3219 cm^{-1} (m), $\nu_{C=N}$ 1619 cm^{-1} (s). ^1H NMR (CD_2Cl_2): Amidine ligand, δ 0.51 and 0.80 (m, CH_2, 4H), 2.30 (s, CH_3, 3H), 2.56 (m, C*H*, 1H), 7.07 (br, Pt*NH*, 1H), 8.98 (d, $^3J_{HH}$ = 7.5 Hz, N*H*, 1H). Amine ligand, δ 0.66 and 0.76 (m, CH_2, 4H), 2.55 (m, C*H*, 1H), 5.11 (br, NH_2, 2H, $^2J_{PtH}$ = 48 Hz). ^{13}C {^1H} NMR (CD_2Cl_2): Amidine ligand, δ 6.3 (*C*H_2), 20.7 (*C*H_3), 24.7 (*C*H), 168.8 (*C*=N). Amine ligand, δ = 7.80 (*C*H_2), 25.2 (*C*H).

trans-[Pt(NH$_2$CH(CH$_2$)$_3$CH$_2$)$_2${N(H)=C(CH$_3$)N(H)CH(CH$_2$)$_3$CH$_2$}$_2$]$^{2+}$[Cl$^-$]$_2$ (**2**). Yield 527 mg, 89%. IR: ν_{N-H} 3338 cm^{-1} (m), $\nu_{C=N}$ 1626 cm^{-1} (s). ^1H NMR ($CDCl_3$): Amidine ligand, δ 2.07 and 1.88 (m, N(H)CHCH_2, 4H), 1.89 and 1.55 (m, N(H)CHCH$_2$CH_2, 4H), 2.26 (s, CH_3, 3H), 3.77 (m, C*H*, 1H), 7.06 (br, Pt*NH*, 1H), 8.80 (d, $^3J_{HH}$ = 9.0 Hz, N*H*). Amine ligand, δ 2.03 and 1.58 (m, NH$_2$CHCH_2, 4H), 1.73 and 1.57 (m, NH$_2$CHCH$_2$CH_2, 4H), 3.00 (m, NH$_2$C*H*, 1H), 5.16 (br, NH_2, $^2J_{PtH}$ = 50 Hz). ^{13}C {^1H} NMR ($CDCl_3$): Amidine ligand, δ 20.6 (*C*H_3), 23.9 (N(H)CHCH$_2$*C*H$_2$), 32.7 (N(H)CH*C*H$_2$), 56.1 (*C*H), 166.3 (*C*=N). Amine ligand, δ 33.9 (NH$_2$CH*C*H$_2$), 23.5 (NH$_2$CHCH$_2$*C*H$_2$), 57.5 (NH$_2$*C*H). ^{15}N NMR: δ −376.3 (NH_2, $^1J_{NH}$ = 73 Hz); −270.1 (PtN*H*, $^1J_{NH}$ = 80 Hz); −256.4 (N*H*, $^1J_{NH}$ = 90 Hz). ^{195}Pt NMR: δ −3487.

trans-[Pt(NH$_2$CH(CH$_2$)$_4$CH$_2$)$_2${N(H)=C(CH$_3$)N(H)CH(CH$_2$)$_4$CH$_2$}$_2$]$^{2+}$[Cl$^-$]$_2$ (**3**). Yield 557 mg, 87%. IR (KBr): ν_{N-H} 3223, 3079 cm^{-1} (m), $\nu_{C=N}$ 1619 cm^{-1} (s). ^1H NMR ($CDCl_3$): Amidine ligand, δ 1.68 and 2.00 (m, N(H)CHCH_2, 4H), 1.22 and 1.80 (m, N(H)CHCH$_2$CH_2, 4H), 1.17 and 1.68 (m, N(H)CHCH$_2$CH$_2$CH_2, 2H), 3.11 (m, C*H*, 1H); 2.23 (s, CH_3, 3H), 6.91 (br, Pt*NH*), 8.71 (d, $^3J_{HH}$ = 9.6 Hz, N*H*). Amine ligand, δ 1.19 and 2.25 (m, NH$_2$CHCH_2, 4H), 1.18 and 1.56 (m, NH$_2$CHCH$_2$CH_2, 4H), 1.22 and 1.55 (m, NH$_2$CHCH$_2$CH$_2$CH_2, 2H), 2.35 (m, NH$_2$C*H*, 1H), 4.86 (s, NH_2, $^2J_{PtH}$ = 54 Hz). ^{13}C {^1H} NMR ($CDCl_3$): Amidine ligand, δ 20.6 (*C*H_3), 25.77 (N(H)CHCH$_2$*C*H$_2$), 24.9 (N(H)CHCH$_2$*C*H$_2$), 33.3 (N(H)CH*C*H$_2$), 54.3 (*C*H), 165.4 (*C*=N). Amine ligand, δ 25.3 (NH$_2$CHCH$_2$*C*H$_2$), 24.7 (NH$_2$CHCH$_2$CH$_2$*C*H$_2$), 34.3 (NH$_2$CH*C*H$_2$), 54.9 (NH$_2$*C*H).

X-ray Measurements and Structure Determination for *trans*-[Pt(NH$_2$CHCH$_2$CH$_2$)$_2${N(H)=C(CH$_3$)N(H)CHCH$_2$CH$_2$}$_2$]$^{2+}$[Cl$^-$]$_2$ (1). Crystal was lodged in Lindemann glass capillary and centered on a four circle Philips PW1100 diffractometer using graphite monochromated Mo Kα radiation (0.71073 Å), following the standard procedures at room temperature. All intensities were corrected for Lorentz polarization and absorption.[123] The structures were solved by standard direct methods.[124] Refinement was carried out by full-matrix least-squares procedures (based on F_o^2) using anisotropic temperature factors for all non-hydrogen atoms. Hydrogen atoms were observed via the difference Fourier map and refined isotropically, excepted those of the C(2), C(3), C(5), C(7), and C(8) carbon atoms, which were placed in calculated positions with fixed isotropic thermal parameters (1.2 U_{equiv}) of the parent carbon atom. Structure refinement and final geometrical calculations were carried out with SHELXL-97[125] program, implemented in the WinGX package.[126] Crystallographic data for **1** have been deposited with the Cambridge Crystallographic Data Centre as supplementary publications no. CCDC 742859. Copies of the available material can be obtained, free of charge from CCDC, 12 Union Road, Cambridge CH2 1EZ, UK (fax +44-1223-336033 or e-mail: deposit@ccdc.cam.ac.uk or http://www.ccdc.cam.ac.uk).

Biological Assays. Platinum(II) bis-amidine derivatives were dissolved in water, DMSO, PEG400, or PEGDME500 just before the experiment and a calculated amount of drug solution (50, 25, 12.5, 6.25, 3.125 μM) was added to the growth medium containing cells to a final solvent concentration of 0.5%, which had no discernible effect on cell killing. MTT (3-(4,5-dimethylthiazol-2-yl)-2,5-diphenyltetrazolium bromide), cisplatin, transplatin, and doxorubicin were obtained from Sigma Chemical Co., St. Louis, MO.

Cell Cultures. Human lung (A549), breast (MCF-7), cervix (HeLa), and colon (HCT-15) carcinoma along with melanoma (A375) cell lines and HFF-1 human normal fibroblasts were obtained by ATCC, Rockville, MD. 2008, its cisplatin resistant variant, C13*, and ciplatin-revertant phenotype RH4, are human ovarian cancer cell lines, kindly provided by Prof. G. Marverti (Department of Biomedical Science of Modena University, Italy). LoVo human colon-carcinoma cell line and its derivative multidrug-resistant subline (LoVo MDR) were kindly provided by Prof. F. Majone (Department of Biology of Padova University, Italy). A2780 and its multidrug-resistant phenotype, A2780 ADR, are human ovarian adenocarcinoma cell lines kindly provided by Prof. N. Colabufo (Department Farmaco-Chimico of Bari University, Italy). Cell lines were maintained in the logarithmic phase at 37 °C in a 5% carbon dioxide atmosphere using the following culture media containing 10% fetal calf serum (Euroclone, Milan, Italy), antibiotics (50 units·mL^{-1} penicillin and 50 μg·mL^{-1} streptomycin) and 2 mM L-glutamine: (i) RPMI-1640 medium (Euroclone) with 25 mM HEPES buffer for MCF-7, HCT-15, A2780, A2780 ADR, 2008, C13*, and RH4 cells, (ii) F-12 HAM'S (Sigma Chemical Co.) for LoVo and LoVo MDR cells (LoVo MDR culture medium also contained 0.1 μg·mL^{-1} doxorubicin), (iii) D-MEM medium (Euroclone) for A549, A375 and HFF-1 cells.

Cytotoxicity Assay. The growth inhibitory effect toward tumor cell lines was evaluated by means of MTT (tetrazolium salt reduction) assay.[127] Briefly, between 3 and 8 × 10^3 cells, dependent upon the growth characteristics of the cell line, were seeded in 96-well microplates in growth medium (100 μL) and then incubated at 37 °C in a 5% carbon dioxide atmosphere. After 24 h, the medium was removed and replaced with fresh media containing the compound to be studied at the appropriate concentration. Triplicate cultures were established for each treatment. After 48 h, each well was treated with 10 μL of a 5 mg·mL^{-1} MTT (3-(4,5-dimethylthiazol-2-yl)-2,5-diphenyltetrazolium bromide) saline solution, and after 5 h of incubation, 100 μL of a sodium dodecylsulfate (SDS) solution in HCl (0.01 M) was added. After overnight incubation in the dark at 37 °C in a 5% carbon dioxide atmosphere, the inhibition of cell growth induced by tested compounds was detected by measuring the absorbance of each well at 570 nm using a Bio-Rad 680 microplate reader (Milan, Italy). Mean absorbance for each drug dose was expressed as a percentage of the control untreated well absorbance and plotted vs drug concentration. IC_{50} values represent the drug concentrations that reduced the mean absorbance at 570 nm to 50% of those in the untreated control wells.

Flow Cytometric Analysis. Drug-induced cell cycle effects and DNA fragmentation were analyzed by flow cytometry after DNA staining with propidium iodide (PI), according to Nicoletti et al.[108] Briefly, 2008 cells (5 × 10^5 cells) were exposed for 24 h to tested compound concentrations corresponding to IC_{50} values. One mL of a PI solution, containing 50 μg/mL of PI, 0.1% m/v of Triton X-100, and 0.01% m/v of sodium citrate, was added to the cells and then incubated for 25 min at 4 °C in the dark. Induced cell death was determined as a percentage of hypodiploid nuclei counted out of the total cell population, measured on a FACSCalibur flow cytometer (Becton-Dickinson, Franklin Lakes, NJ) on a 550−600 nm filter. Analysis was performed by Cell Quest software (Becton-Dickinson).

Caspase-3 Activity. Caspase-3 activity was detected with the ApoAlert Caspase-3 Fluorescent Assay Kit (Clontech, Mountain View, CA) according to the producer's recommended procedures. In the amount of 10^6, 2008 cells were collected

following 12 or 24 h of incubation of tested compounds (at concentrations corresponding to IC_{50} values) and lysed on ice in 50 μL of lysis buffer for 10 min and then treated with 50 μL of reaction buffer containing dithiothreitol (DTT) and 5 μL of caspase-3 substrate solution (Asp-Glu-Val-Asp-7-amino-4-trifluoromethyl-coumarin [DEVD-AFC], Clontech). Fluorescence was determined on a Perkin-Elmer 550 spectrofluorometer (excitation 440 nm, emission 505 nm). Caspase-3 activity was expressed as the increase in AFC-emitted fluorescence. Student's *t* test was used for data analysis.

Reverse-Transcriptase and Polymerase Chain Reaction (RT-PCR). Total RNA was isolated using TRI Reagent (Sigma-Aldrich) according to manufacture's instructions. RNA quantification was performed spectrophotometrically (wavelengths of 260 vs 280 nm). Synthesis of cDNA was performed by first strand reverse transcription method with 5 μg of total RNA by MLV reverse transcriptase kit (Promega) and nonamere random primers (final concentration 0.69 pMol) according to manufacture's instructions.

Semiquantitative PCR was then used to compare the total levels of p53 mRNA. Briefly, to 2 μL of cDNA was added 5 μL of PCR buffer 10X (Genecraft), 2.5 mM $MgCl_2$ (Genecraft), 0.2 mM dNTPs (Genecraft), 100 pMol of each specific primer (p53: forward AGGGAGCACTAAGCGAGCAC and reverse AACATGAGTTTTTTATGGCGGG; β-actin forward 5′TGACGGGGTCACCCACACTGTGCCCATCTA3′ and reverse 5′-GAAGTAGTAAGTGGGAACCGTGT3′) (MWG-operon), 4 μL of a mix of primer−competimers (1:7) specific for the quantitation of the 18s RNA as internal standard (Ambion) and 2.5U of Taq polymerase (Genecraft). Thermal cycling consisted of 2 min at 94 °C followed by 35 cycles composed by 30 s at 94 °C, 1 min at 59 °C, and 1 min at 72 °C. PCR products were electrophoresed in a 2.5% agarose gel (Sigma) and visualized after ethidium bromide staining. Electrophoresis images were analyzed by Image Quant Software (Molecular Dynamics).

Western Blotting Analysis. After treatment of 2008 cells (10^6) with IC_{50} concentrations of tested compounds, cells were harvested, lysed (2% SDS, 0.06 M Tris−HCl pH 6.8), and protein concentrations determined following Lowry assay.[128] Protein (35 μg) was electrophoresed on a 12% polyacrylamide gel and the gel blotted onto nitrocellulose membrane using the semidry blot system at 2 mA/cm^2 for 60 min in 25 mM Tris-HCl, pH 8.3, 192 mM glycine, and 20% methanol. The membrane was blocked overnight at room temperature with a blocking reagent (20 mM Tris, pH 7.4, 0.2% Tween-20, 125 mM NaCl, 0.1% sodium azide, and 4% nonfat dry milk). Then it was incubated for 1 h with the primary antibody (mouse antihuman p53 antibody, 1:5000, mouse antihuman β-actin antibody, 1:500, Abcam, UK). After incubation with antimouse secondary antibody (1:3000 Abcam, UK), signals were detected by enhanced chemiluminescence system (Amersham, United Kingdom).

Evaluation of DNA Damage with Alkaline Single-Cell Gel Electrophoresis Assay (Comet Assay). 2008 (10^5) cells were seeded in 25 cm^2 flasks in growth medium (6 mL). After 24 h, cells were incubated for different exposure times (6, 12, 24, and 48 h) with IC_{50} of tested compounds (followed by treatment with H_2O_2 1 μM for 30 min in modified comet assay experiments for cross-link determination).[129] Subsequently, cells were washed twice with cold PBS, harvested, centrifuged, and resuspended at 1×10^5 cell·mL^{-1} in 1% low melting point agarose (LMPA, Trevigen). Then 50 μL of cells−LMPA mixture was layered onto frosted microscope slides, which were precoated with 1% normal agarose. After the agar had been allowed to set at 4 °C, the slides were immersed in lysis buffer (100 mM Na_2EDTA, 2.5 M NaCl, 10 mM Tris pH 10.0, and 1% Triton X-100) for 1 h at 4 °C. The slides were then incubated in an alkaline electrophoresis solution (1 mM EDTA, 300 mM NaOH, pH > 13) at 4 °C for 40 min, followed by electrophoresis (1 V·cm^{-1}) at 4 °C for 30 min. The slides were washed with neutralization buffer three times before immersion in absolute ethanol for 20 min and air-dried at room temperature. The DNA was stained with SYBR Green (1 μg/mL) for 5 min at 4 °C. A total of 50 comets per slide, randomly captured at the constant depth of the gel, were examined at 40× magnification in a fluorescence microscope (Olympus BX41; excitation, 495 nm; emission, 521 nm) connected through a black and white camera to a computer-based image analysis system. Comets were randomly captured at a constant depth of the gel, avoiding the edges of the gel, occasional dead cells, and superimposed comets. DNA damage was measured as tail length (distance of DNA migration from the center of the body of the nuclear core), tail moment (tail length × % of DNA in the tail) using Cell-F software (Olympus).

Animals and Tumor Cells. All studies involving animal testing were carried out in accordance with the ethical guidelines for animal research adopted by the University of Padova, acknowledging the Italian regulation and the European Directive 86/609/EEC as to the animal welfare and protection and the related codes of practice. Mice provided by the Charles River, Italy, were housed in steel cages under controlled environmental conditions (constant temperature, humidity, and 12 h dark−light cycle) and alimented with commercial standard feed and tap water ad libitum. Animals were observed daily, and body weight and food intake recorded. Lewis lung carcinoma cell (LLC) line was purchased from (ECACC, UK). LLC line was maintained in D-MEM (Euroclone) supplemented with 10% heat-inactivated FBS (Euroclone), 10 mM L-glutamine, 100 U/mL penicillin, and 100 μg/mL streptomycin in a 5% CO_2 air incubator at 37 °C.

Acute Toxicity Studies. Six-week old both male and female BALB/c mice (weighting 18 ± 2 g each) were randomly divided into groups of eight animals per toxic dose and treated with a single ip injection of **3** (2.5/5/10/20/50/100 mg kg^{-1} in 1% v/v PEG400/PBS). The animals were observed for 24 h for signs of toxicity and mortality. The LD_{50} dose (LD = lethal dose) was estimated by probit analysis and linearity assessed by $\chi 2$ test ($p < 0.005$). Lethality is expressed as LD_{50} value in terms of milligrams of tested compound per mouse weight (kg).

In Vivo Anticancer Activity toward Lewis Lung Carcinoma. Lewis lung carcinoma (LLC) was implanted im as a 2×10^6 cells inoculum into the right hind leg of 8-week old male and female C57BL mice (24 ± 3 g body weight). After 24 h from tumor implantation, mice were randomly divided into five groups (8 animals per group, 10 controls) and treated with an ip injection of **3** (3/6/12 mg kg^{-1} in 1% v/v PEG400/PBS), cisplatin (1.5 mg kg^{-1} in PBS), or the vehicle solution (1% v/v PEG400/PBS, control) on days 3, 5, 7, 9, 11, and 13 after tumor inoculation. At day 15, animals were sacrificed, the legs were amputated at the proximal end of the femur, and the inhibition of tumor growth was determined according to the difference in weight of the tumor-bearing leg and the healthy leg of the animals expressed as % referred to the control animals. Body weight was measured every two days and was taken as a parameter of systemic toxicity.

Statistical Analysis. All the values are the means ± SD of not less than three measurements. For in vitro studies, multiple comparisons were made by one-way analysis of variance followed by ANOVA. For in vivo experiments, statistical analysis was carried out using the Student's *t* test

Acknowledgment. This work was financially supported by the University of Padova (Progetto di Ateneo CPDA065113/06) and by the Ministero dell'Istruzione dell'Università e della Ricerca (PRIN 20078EWK9B). We are grateful to CIRCMSB (Consorzio Interuniversitario di Ricerca in Chimica dei Metalli nei Sistemi Biologici).

Supporting Information Available: Elemental analyses; fragmentation pathways of compounds **1**, **2**, and **3** dissolved in CH_3CN under ESI conditions; crystal data and structure refinement parameters; selected bond lengths and angles; crystal packing; crystallographic details in the form of a CIF file. This material is available free of charge via the Internet at http://pubs.acs.org.

References

(1) Kalinowska-Lis, U.; Ochocki, J.; Matlawska-Wasowska, K. Trans geometry in platinum antitumor complexes. *Coord. Chem. Rev*. **2008**, *252*, 1328–1345.

(2) Coluccia, M.; Natile, G. *trans*-Platinum complexes in cancer therapy. *Anti-Cancer Agents Med. Chem*. **2007**, *7*, 111–123.

(3) Natile, G.; Coluccia, M. Current status of *trans*-platinum compounds in cancer therapy. *Coord. Chem. Rev*. **2001**, *216*, 383–410.

(4) Hambley, T. W. The influence of structure on the activity and toxicity of Pt anti-cancer drugs. *Coord. Chem. Rev*. **1997**, *166*, 181–223.

(5) Leng, M.; Schwartz, A.; Giraud Panis, M. J. Transplatin-modified oligonucleotides as potential antitumor drugs. In *Platinum Based Drugs in Cancer Therapy*; Kelland, L. R., Farrell, N. P., Eds.; Humana Press, Totowa, NJ, 2000; pp 63−85.

(6) Liu, Y.; Vinje, J.; Pacifico, C.; Natile, G.; Sletten, E. Formation of adenine-N3/guanine-N7 cross-link reaction of trans oriented platinum substrates with dinucleotides. *J. Am. Chem. Soc*. **2002**, *124*, 12854–12862.

(7) Berners-Price, S.; Appleton, T. G. The chemistry of cisplatin in aqueous solution. In *Platinum Based Drugs in Cancer Therapy*; Kelland, L. R., Farrell, N. P., Eds.; Humana Press, Totowa, NJ, 2000; pp 3−35.

(8) Brabec, V. Chemistry and structural biology of 1,2-interstrand adducts of cisplatin. In *Platinum Based Drugs in Cancer Therapy*; Kelland, L. R., Farrell, N. P., Eds.; Humana Press, Totowa, NJ, 2000; pp 37−61.

(9) O'Neill, C. F.; Hunakova, L.; Kelland, L. R. Cellular pharmacology of cis and trans pairs of platinum complexes in cisplatin-sensitive and -resistant human ovarian carcinoma cells. *Chem.−Biol. Interact*. **1999**, *123*, 11–29.

(10) Farrell, N.; Ha, T. T. B.; Souchard, J. P.; Wimmer, F. L.; Cros, S.; Johnson, N. P. Cytostatic *trans*-platinum(II) complexes. *J. Med. Chem*. **1989**, *32*, 2240–2241.

(11) Chen, Y.; Guo, Z.; Parson, S.; Sadler, P. J. Stereospecific and kinetic control over the hydrolysis of a sterically hindered platinum picoline anticancer complex. *Chem. Eur. J*. **1998**, *4*, 672–676.

(12) Knipp, M.; Karotki, A. V.; Chesnov, S.; Natile, G.; Sadler, P. J.; Brabec, V.; Vasak, M. Reaction of Zn_7metallothionein with *cis*- and *trans*-[Pt(N-donor)$_2$Cl$_2$] anticancer complex: trans Pt^{II} complexes retain their N-donor ligands. *J. Med. Chem*. **2007**, *50*, 4075–4086.

(13) Zou, Y.; Van Houten, B.; Farrell, N. Ligand effects in platinum binding to DNA. A comparison of DNA binding properties for *cis*- and *trans*-[PtCl$_2$(amine)$_2$](amine = NH_3, pyridine). *Biochemistry* **1993**, *32*, 9632–9638.

(14) Van Beusichem, M.; Farrell, N. Activation of the trans geometry in platinum antitumor complexes. Synthesis, characterization, and biological activity of complexes with the planar ligands pyridine, *N*-methylimidazole, thiazole, and quinoline. Crystal and molecular structure of *trans*-dichlorobis(thiazole)platinum-(II). *Inorg. Chem*. **1992**, *31*, 634–639.

(15) Montero, E. I.; Diaz, S.; Gonzalez-Vadillo, A. M.; Perez, J. M.; Alonso, C.; Navarro-Ranninger, C. Preparation and characterization of novel *trans*-[PtCl$_2$(amine)(isopropylamine)] compounds: cytotoxic activity and apoaptosis induction in *ras*-transformed cells. *J. Med. Chem*. **1999**, *42*, 4264–4268.

(16) Perez, J. M.; Montero, E. I.; Gonzalez, A. M.; Solans, X.; Font-Bardia, M.; Fuertes, M. A.; Alonso, C.; Navarro-Ranninger, C. X-ray structure of cytotoxic *trans*-[PtCl$_2$(dimethylamine)-(isopropylamine)]: interstrand cross-link efficiency, DNA sequence specificity, and inhibition of the B−Z transition. *J. Med. Chem*. **2000**, *43*, 2411–2418.

(17) Coluccia, M.; Nassi, A.; Loseto, F.; Boccarelli, A.; Mariggiò, M. A.; Giordano, D.; Intini, F. P.; Caputo, P. A.; Natile, G. A *trans*-platinum complex showing higher antitumor activity than the cis congeners. *J. Med. Chem*. **1993**, *36*, 510–512.

(18) Boccarelli, A.; Giordano, D.; Natile, G.; Coluccia, M. Differential processing of antitumor-active and antitumor-inactive *trans*-platinum compounds by SKOV-3 ovarian cancer cells. *Biochem. Pharmacol*. **2006**, *72*, 280–292.

(19) Novakova, O.; Kasparkova, J.; Malina, J.; Natile, G.; Brabec, V. DNA-protein cross-limking by *trans*-[PtCl$_2$(*E*-iminoether)$_2$]. A concept for activation of the trans geometry in platinum antitumor complexes. *Nucleic Acids Res*. **2003**, *31*, 6450–6460.

(20) Ramos-Lima, F. J.; Quiroga, A. G.; Garcia-Senelde, B.; Blanco, F.; Carnero, A.; Navarro-Ranninger, C. New *trans*-platinum drugs with phosphines and amines carrier ligands induce apoptosis in tumor cells resistant to cisplatin. *J. Med. Chem*. **2007**, *50*, 2194–2199.

(21) Zorbas-Seifried, S.; Jakupec, M. A.; Kukushkin, N. V.; Groessl, M.; Hartinger, C. G.; Semenova, O.; Zorbas, H.; Yu Kukushkin, V.; Keppler, B. K. Reversion of structure−activity relationship of antitumor platinum complexes by acetoxime but not hydroxylamine ligands. *Mol. Pharmacol*. **2007**, *71*, 357–365.

(22) Kelland, L. R.; Barnard, C. F. J.; Mellish, K. J.; Jones, M.; Goddard, P. M.; Valenti, M.; Bryant, A.; Murrer, B. A.; Harrap, K. R. A novel *trans*-platinum coordination complex possessing in vitro and in vivo antitumor activity. *Cancer Res*. **1994**, *54*, 5618–5622.

(23) Giandomenico, C. M.; Abrams, M. J.; Murrer, B. A.; Vollano, J. F.; Rheinheimer, M. I.; Wyer, S. B.; Bossard, G. E.; HigginsIII, J. D. Carboxylation of kinetically inert platinum(IV) hydroxy complexes. An entrée into orally active platinum(IV) antitumor agents. *Inorg. Chem*. **1995**, *34*, 1015–1021.

(24) Mellish, K. J.; Barnard, C. F. J.; Murer, B. A.; Kelland, L. R. DNA-binding properties of novel *cis*- and *trans*-platinum-based anticancer agents in 2 human ovarian carcinoma cell lines. *Int. J. Cancer* **1995**, *62*, 717–723.

(25) Kelland, L. R.; Barnard, C. F. J.; Evans, I. G.; Murrer, B. A.; Theobald, B. R. C.; Wyer, S. B.; Goddard, P. M.; Jones, M.; Valenti, M.; Bryant, A.; Rogers, P. M.; Harrap, K. R. Synthesis and in vitro and in vivo antitumor activity of a series of *trans*-platinum antitumor complexes. *J. Med. Chem*. **1995**, *38*, 3016–3024.

(26) Gonzalez-Vadillo, A. M.; Alvarez-Valdes, A.; Moneo, V.; Blanco, F.; Diaz, R. G.; Carnero, A.; Navarro-Ranninger, C. Structure−activity relationship of new *trans*-platinum(II) and (IV) complexes with cyclohexylamine. Interference with cell cycle progression and induction of cell death. *J. Inorg. Biochem*. **2007**, *101*, 551–558.

(27) Perez, J. M.; Kelland, L. R.; Montero, E. I.; Boxall, F. E.; Fuertes, M. A.; Alonso, C.; Navarro-Ranninger, C. Antitumor and cellular pharmacological properties of a novel platinum(IV) complex: *trans*-[PtCl$_2$(OH)$_2$(dimethylamine)(isopropylamine)]. *Mol. Pharmacol*. **2003**, *63*, 933–944.

(28) Kelland, L. R.; Abel, G.; McKeage, M. L.; Jones, M.; Goddard, P. M.; Valenti, M.; Murrer, B. A. Preclinical antitumor evaluation of bis-acetato-ammine-dichloro-cyclohexylamine platinum(IV): an orally active platinum drug. *Cancer Res*. **1993**, *53*, 2581–2586.

(29) Wheate, W. J.; Day, A. I.; Blanch, R. J.; Arnold, A. P.; Cullinane, C.; Collins, J. G. Multinuclear platinum complexes encapsulated in cucurbit[n]uril as an approach to reduce toxicity in cancer treatment. *Chem. Commun*. **2004**, 1424–1425.

(30) Marini, V.; Kasparkova, J.; Novakova, O.; Monsù Scolaro, L.; Romeo, R.; Brabec, V. Biophysical analysis of natural, double-helical DNA modified by a dinuclear platinum(II) organometallic compound in a cell-free medium. *J. Biol. Inorg. Chem*. **2002**, *7*, 725–734.

(31) Cox, J. W.; Berners-Price, S. J.; Davies, M. S.; Qu, Y.; Farrell, N. Kinetic analysis of the stepwise formation of a long-range DNA interstrand cross-link by a dinuclear platinum antitumor complex: evidence for aquated intermediates and formation of both kinetically and thermodynamically controlled conformers. *J. Am. Chem. Soc*. **2001**, *123*, 1316–1326.

(32) Farrell, N. Polynuclear charged platinum compounds as a new class of anticancer agents. In *Platinum Based Drugs in Cancer Therapy*; Kelland, L. R., Farrell, N. P., Eds.; Humana Press, Totowa, NJ, 2000; pp 321−338.

(33) Hollis, L. S.; Amundsen, A. R.; Stern, E. W. Chemical and biological properties of a new series of *cis*-diammineplatinum(II) antitumor agents containing three nitrogen donors: *cis*-[Pt-(NH_3)$_2$(N-donor)Cl]$^+$. *J. Med. Chem*. **1989**, *32*, 128–136.

(34) Najajreh, Y.; Ardeli-Tzaraf, Y.; Kasparkova, J.; Heringova, P.; Prilutski, D.; Balter, L.; Jawbry, S.; Khazanov, E.; Perez, J. M.; Barenholz, Y.; Brabec, V.; Gibson, D. Interactions of platinum complexes containing cationic, bicyclic, nonplanar piperidinopiperidine ligands with biological nucleophiles. *J. Med. Chem*. **2006**, *49*, 4674–4683.

(35) Najajreh, Y.; Perez, J. M.; Navarro-Ranninger, C.; Gibson, D. Novel soluble cationic *trans*-diaminedichloroplatinum(II) complexes that are active against cisplatin resistant ovarian cancer cell lines. *J. Med. Chem*. **2002**, *45*, 5189–5195.

(36) Aris, S. M.; Gewirtz, D. A.; Ryan, J. J.; Knott, K. M.; Farrell, N. P. Promotion of DNA strand breaks, interstrand cross-links and apoptotic cell death in A2780 human ovarian cancer cells by transplatinum planar amine complexes. *Biochem. Pharmacol.* **2007**, *73*, 1749–1757.

(37) Muller, J.; Drumm, M.; Boudvillain, M.; Leng, M.; Sletten, E.; Lippert, B. Parallel-stranded DNA with Hoogsteen base pairing stabilized by a *trans*-$[Pt(NH_3)_2]^{2+}$ cross-link: characterization and conversion into a homodimer and a triplex. *J. Biol. Inorg. Chem.* **2000**, *5*, 603–611.

(38) Boudvillain, M.; Guerin, M.; Dallies, R.; Saison-Behmoaras, T.; Leng, M. Transplatin-modified oligo(2′-*O*-methyl ribonucleotide)s: a new tool for selective modulation of gene expression. *Biochemistry* **1997**, *36*, 2925–2931.

(39) Marzano, C.; Mazzega Sbovata, S.; Bettio, F.; Michelin, R. A.; Seraglia, R.; Kiss, T.; Venzo, A.; Bertani, R. Solution behaviour and biological activity of bisamidine complexes of platinum(II). *J. Biol. Inorg. Chem.* **2007**, *12*, 477–493.

(40) Mazzega Sbovata, S.; Bettio, F.; Marzano, C.; Mozzon, M.; Bertani, R.; Benetollo, F.; Michelin, R. A. Benzylamidine complexes of platinum(II) derived by nucleophilic addition of primary and secondary amines. X-ray crystal structure of *trans*-$[PtCl_2\{Z\text{-}N(H)=C(NHMe)CH_2Ph\}_2]$. *Inorg. Chim. Acta* **2008**, *361*, 3109–3116.

(41) Mazzega Sbovata, S.; Bettio, F.; Mozzon, M.; Bertani, R.; Venzo, A.; Benetollo, F.; Michelin, R. A.; Gandin, V.; Marzano, C. Cisplatin and transplatin complexes with benzyliminoether ligands: synthesis, characterization, structure−activity relationships, and in vitro and in vivo antitumor efficacy. *J. Med. Chem.* **2007**, *50*, 4775–4784.

(42) Reedijk, J. Why does cisplatin guanine-N7 with competing S-donor ligands available in the cell? *Chem. Rev.* **1999**, *99*, 2499–2510.

(43) Najajreh, Y.; Khazanov, E.; Jawbry, S.; Ardeli-Tzaraf, J.; Perez, M. Y.; Kasparkova, J.; Brabec, V.; Barenholz, Y.; Gibson, D. Cationic nonsymmetric transplatinum complexes with piperidinopiperidine ligands. Preparation, characterization, in vivo cytotoxicity, in vivo toxicity, and anticancer efficacy studies. *J. Med. Chem.* **2006**, *49*, 4665–4673.

(44) Wei, M.; Cohen, S. M.; Silverman, A. P.; Lippard, J. J. Effects of spectator ligands on the specific recognition of intrastrand platinum DNA cross-links by high mobility group box and TATA-binding proteins. *J. Biol. Chem.* **2001**, *276*, 38774–38780.

(45) Najajreh, Y.; Peleg-Shulman, T.; Moshel, O.; Farrell, N.; Gibson, D. Ligand effects on the binding of *cis*-and *trans*-$[PtCl_2Am_1Am_2]$ to proteins. *J. Biol. Inorg. Chem.* **2003**, *8*, 167–175.

(46) Nayajreh, Y.; Prilutski, D.; Ardeli-Tzaraf, Y.; Perez, J. M.; Khozanov, E.; Barenholz, Y.; Kasparkova, J.; Brabec, V.; Gibson, D. Structure and unique interactions with DNA of a cationic *trans*-platinum complex with the nonplanar bicyclic piperidinopiperidine ligand. *Angew. Chem., Int. Ed.* **2005**, *44*, 2885–2887.

(47) Lee, Y. A.; Won Kang, S.; Yul Park, Y.; Jung, O. S. Chelate vs monodentate amine effects. Direct comparison of bis(acetate) amminedichloro(cyclohexylemine)platinum(IV) (JM216) with its *N*-cyclohexyl-1,3-propanediamine analogue. *J. Mol. Struct.* **2003**, *659*, 129–133.

(48) Khazanov, E.; Berenholz, Y.; Gibson, D.; Najajreh, Y. Novel apoptosis-inducing *trans*-platinum piperidine derivatives: synthesis and biological characterization. *J. Med. Chem.* **2002**, *45*, 5196–5204.

(49) Skander, M.; Retailleau, P.; Bourriè, B.; Schio, L.; Mailliet, P.; Marinetti, A. N. Heterocyclic carbene-amine Pt(II) complexes, a new chemical space for the development platinum-based anticancer drugs. *J. Med. Chem.* **2010**, *53*, 2146–2154.

(50) Khokhar, A. R.; Deng, Y.; Al-Baker, S.; Yoshida, M.; Siddik, Z. H. Synthesis and antitumor activity of ammine/amine platinum(II) and (IV) complexes. *J. Inorg. Biochem.* **1993**, *51*, 677–687.

(51) Zhang, J.; Yong, S. Synthesis, cytotoxicity, and DNA-binding levels of ammine/cyclohexylamine platinum(II) complexes with dicarboxylates. *Synth. React. Inorg., Met.-Org., Nano-Met. Chem.* **2006**, *36*, 345–351.

(52) Burchenal, J. H.; Kalaher, K.; O'Toole, T.; Chisholm, J. Lack of cross-resistance between certain platinum coordination compounds in mouse leukaemia. *Carcer Res.* **1977**, *37*, 3455–3457.

(53) O'Dwyer, P.; Stevenson, J. P.; Johnson, S. W. Clinical experience. DACH-Based Platinum Druds. In *Platinum Based Drugs in Cancer Therapy*; Kelland, L. R., Farrell, N. P., Eds.; Humana Press, Totowa, NJ, 2000; pp 231−249.

(54) Lemma, K.; Shi, T.; Elding, L. I. Kinetics and mechanism for reduction of the anticancer prodrug *trans*,*trans*,*trans*-[Pt(OH)(*c*-CHNH)(NH)] (JM335) by thiols. *Inorg. Chem.* **2000**, *39*, 1728–1734.

(55) O'Neill, C. F.; Ormerod, M. G.; Robertson, D.; Titley, J. C.; Cumber-Walsweer, Y.; Kelland, L. R. Apoptotic and nonapoptotic cell death induced by *cis* and *trans* analogues of a novel ammine(cyclohexylamine)dihydroxodichloroplatinum(IV) complex. *Br. J. Cancer* **1996**, *74*, 1037–1045.

(56) Holford, J.; Beale, P. J.; Boxall, F. E.; Sharp, S. Y.; Kelland, L. R. Mechanism of drug resistance to the platinum complex ZD0473 in ovarian cancer cell lines. *Eur. J. Cancer* **2000**, *36*, 1984–1990.

(57) Kelland, L. R.; Sharp, S. Y.; O'Neill, C. F.; Raynaud, F. I.; Beale, P. J.; Judson, I. R. Mini-review: discovery and development of platinum complexes designed to circumvent cisplatin resistance. *J. Inorg. Biochem.* **1999**, *77*, 111–115.

(58) Fokkema, E.; Groen, H. J. M.; Helder, M. N.; deVries, E. G. E.; Meijer, C. JM216-, JM218, and cisplatin-induced cytotoxicity in relation to platinum DNA adduct formation, glutathione levels and p53 status in human tumour cell lines with different sensitivities to cisplatin. *Biochem. Pharmacol.* **2002**, *63*, 1989–1996.

(59) Silverman, A. P.; Bu, W.; Cohen, S. M.; Lippard, S. J. 2.4 Å Crystal structure of the asymmetric platinum complex $\{Pt(ammine)(cyclohexylamine)\}^{2+}$ bound to a dodecamer DNA duplex. *J. Biol. Chem.* **2002**, *277*, 49743–49749.

(60) Kelland, L. Broadening the clinical use of platinum drug-based chemotherapy with new analogues satraplatin and picoplatin. *Expert Opin. Invest. Drugs* **2007**, *16*, 1009–1021.

(61) Cepero, V.; Garcia-Serrelde, B.; Moneo, V.; Blanco, F.; Gonzalez-Vadillo, A. M.; Alvarez-Valdes, A.; Navarro-Ranninger, C.; Carnero, A. *trans*-Platinum(II) complexes with cyclohexylamine as expectator ligand induce necrosis in tumour cells by inhibiting DNA synthesis and RNA transcription. *Clin. Transl. Oncol.* **2007**, *9*, 521–530.

(62) Leng, M.; Locker, D.; Giraud, M. J.; Schwartz, A.; Intini, F. P.; Natile, G.; Pisano, C.; Boccarelli, A.; Giordano, D.; Coluccia, M. Replacement of an NH_3 by an iminoether in transplatin makes an antitumor drug from an inactive compound. *Mol. Pharmacol.* **2000**, *58*, 1525–1535.

(63) Bertani, R.; Michelin, R. A.; Venzo, A.; Mozzon, M.; Mazzega Sbovata, S. Reactivity of *trans*-$PtCl_2(NCMe)_2$ with cycloaliphatic amines: an ESI and NMR study. X ray structure of *trans*-$[PtCl_2\{N(H)=C(CH_3)NH\overline{CHCH_2CH_2}\}_2]$. *Inorg. Chim. Acta* **2010**, *363*, 487–494.

(64) Kauffman, G. B.; Cowan, D. O. *Cis*- and *trans*-dichlorodiammineplatinum(II). *Inorg. Synth.* **1963**, *7*, 239–240.

(65) Natile, G.; Intini, F. P.; Bertani, R.; Michelin, R. A.; Mozzon, M.; Mazzega Sbovata, S.; Venzo, A.; Seraglia, R. Synthesis and characterization of the amidine complexes *trans*-$[PtCl(NH_3)\{HN=C(NH_2)R\}Cl$ (R = Me, Ph, CH_2Ph) derived from addition of NH_3 to the coordinated nitriles in *trans*-$[PtCl_2(N\equiv CR)_2]$. *J. Organomet. Chem.* **2005**, *690*, 2121–2127.

(66) Tschugaeff, L.; Lebedinski, W. Sur deux series de complexes derives du platine bivalent et correspondant a l'indice de coordination. *C.R. H. S. Acad. Sci.* **1915**, *161*, 563–564.

(67) Stephenson, C. The crystal structure of diammine bis(acetamidine)platinum(II) chloride monohydrate, $Pt(NH_3)[CH_3C(NH_2)NH]_2Cl_2\cdot H_2O$. *J. Inorg. Nucl. Chem.* **1962**, *24*, 801–805.

(68) Kukushkin, Y. N.; Kiseleva, N. P.; Zangrando, E.; Kukushkin, V. Y. Formation of two stable seven-membered chelate rings bound to one metal center due to addition of bifunctional amine to coordinated nitriles. *Inorg. Chim. Acta* **1999**, *285*, 203–207.

(69) Belluco, U.; Benetollo, F.; Bertani, R.; Bombieri, G.; Michelin, R. A.; Mozzon, M.; Pombeiro, A. J. L.; Costa Guedes da Silva, F. Stereochemical investigation of the addition of primary and secondary aliphatic amines to the nitrile complexes *cis*- and *trans*-$[PtCl_2(NCMe)_2]$. X-ray structures of the amidine complexes *trans*-$[Pt(NH_2Pr^i)_2\{Z\text{-}N(H)=C(NHPr^i)Me\}]Cl_2\cdot 4H_2O$ and *trans*-$[PtCl_2(NCMe)\{E\text{-}N(H)=C(NMeBu^t)Me\}$. *Inorg. Chim. Acta* **2002**, *330*, 229–239.

(70) Tyan, M. R.; Bokach, N. A.; Wang, M. J.; Haukka, M.; Kuznetsov, M. L.; Kukushkin, V. Y. Facile cyanamide−ammonia coupling mediated by *cis*- and *trans*-$[Pt^{II}L_2]$ centers and giving metal-bound guanidines. *J. Chem. Soc., Dalton Trans.* **2008**, 5178–5188.

(71) Kritzenberger, J.; Zimmermann, F.; Wokaun, A. ^1H NMR and vibrational spectra of *cis*-dichlorobis(cycloalkylamine)-platinum-(II) complexes. *Inorg. Chim. Acta* **1993**, *210*, 47–56.

(72) Rochon, F. D.; Buculei, V. Study of Pt(II)-cyclic amines complexes of the types *cis*-and *trans*-$Pt(amine)_2I_2$ and *cis*- and *trans*-$Pt(amine)_2(NO_3)_2$ and their aqueous products. *Inorg. Chim. Acta* **2005**, *358*, 2040–2056.

(73) Gabano, E.; Marengo, E.; Bobba, M.; Robotti, E.; Cassino, C.; Botta, M.; Osella, D. ^{195}Pt NMR spectroscopy: a chemometric approach. *Coord. Chem. Rev.* **2006**, *250*, 2158–2174.

(74) Mason, J. Nitrogen nuclear magnetic resonance spectroscopy in inorganic, organometallic and bioinorganic chemistry. *Chem. Rev*. **1981**, *81*, 205–227.

(75) von Philipsborn, W.; Muller, R. ^{15}N-NMR spectroscopy: new methods and applications. *Angew. Chem., Int. Ed. Engl*. **1986**, *25*, 383–486.

(76) Duthaler, R. O.; Roberts, J. D. Nitrogen-15 nuclear magnetic resonance spectroscopy. Solvent effects on the ^{15}N chemical shifts of saturated amines and their hydrochlorides. *J. Magn. Reson*. **1979**, *34*, 129–139.

(77) Belluco, U.; Benetollo, F.; Bertani, R.; Bombieri, G.; Michelin, R. A.; Mozzon, M.; Tonon, O.; Pombeiro, A. J. L.; da Silva, F. C. G. Addition reactions of primary and secondary aliphatic amines to the benzonitrile ligands in *cis*- and *trans*-[$PtCl_2$-$(NCPh)_2$] complexes. X-ray structure of the amidine complex *trans*-[$PtCl_2${*Z*-N(H)=C($NHBu^t$)Ph}$_2$]. *Inorg. Chim. Acta* **2002**, *334*, 437–447.

(78) Bertani, R.; Catanese, D.; Michelin, R. A.; Mozzon, M.; Bandoli, G.; Dolmella, A. Reactions of platinum(II)-nitrile complexes with amines. Synthesis, characterization and X-ray structure of the platinum(II)-amidine complex *trans*-[$PtCl_2${*Z*-N(H)=C(NHMe)-Me}$_2$]. *Inorg. Chem. Commun*. **2000**, *3*, 16–18.

(79) Michelin, R. A.; Bertani, R.; Mozzon, M.; Sassi, A.; Benetollo, F.; Bombieri, G.; Pombeiro, A. J. L. Cis addition of dimethylamine to the coordinated nitriles of *cis*- and *trans*-[$PtCl_2(NCMe)_2$]. X-ray structure of the amidine complex *cis*-[$PtCl_2${*E*-N(H)=C(NMe_2)-Me}$_2$]·CH_2Cl_2. *Inorg. Chem. Commun*. **2001**, *4*, 275–280.

(80) Fanizzi, F.; Natile, G.; Maresca, L.; Manotti-Lanfredi, A. M.; Tiripicchio, A. Platinum(IV) complexes containing a cationic amine ligand: crystal structure of [(2-aminoethyl)ammonium]-pentachloroplatinum(IV) monohydrate. *J. Chem. Soc., Dalton Trans*. **1984**, 1467–1470.

(81) Howard-Lock, H. E.; Lyne Lock, C. J.; Turner, G.; Zvagulis, M. The crystal structure and vibrational spectra of *cis*-dichlorobis-(cyclopropylamine)platinum(II), $PtCl_2(C_3H_5NH_2)_2$. *Can. J. Chem*. **1981**, *59*, 2737–2745.

(82) Renn, O.; Lippert, B.; Schollhorn, H.; Thewalt, U. The X-ray structure of *cis*-bis(cyclopropylamine)bis(1-methylthyminato-N^3)-platinum(II) dihydrate, *cis*-$(cpa)_2Pt(1\text{-}MeT)_2\cdot 2H_2O$, and chemistry related to platinum thymine purple. *Inorg. Chim. Acta* **1990**, *167*, 123–130.

(83) Makarycheva-Mikhailova, A. V.; Bokach, N. A.; Kukushkin, V. Y.; Kelly, P. F.; Gilby, L. M.; Kuznetsov, M. L.; Holmes, K. E.; Haukka, M.; Parr, J.; Stonehouse, J. M.; Elsegood, M. R. J.; Pombeiro, A. J. L. Platinum(IV)-mediated nitrile−sulfimide coupling: a route to heterodiazadienes. *Inorg. Chem*. **2003**, *42*, 301–311.

(84) Garnovskii, D. A.; Garnovskaya, E. D.; Uraev, A. I.; Haukka, M.; Eremenko, I. L.; Kukushkin, V. Y. Hetarylamidines derived from Pt(IV)-mediated coupling of nitriles with aminoheterocyles. *Russ. Chem. Bull*. **2006**, *55*, 1632–1635.

(85) Marzano, C.; Mazzega Sbovata, S.; Gandin, V.; Michelin, R. A.; Venzo, A.; Bertani, R.; Seraglia, R. Cytotoxicity of *cis*-platinum-(II) cycloaliphatic amidine complexes: ring size and solvent effects on the biological activity. *J. Inorg. Biochem*. **2009**, *103*, 1113–1119.

(86) Jones, M. M.; Basinger, M. A.; Field, L.; Holscher, M. A. Coadministration of dimethyl sulfoxide reduces cisplatin nephrotoxicity. *Anticancer Res*. **1991**, *11*, 1939–1942.

(87) Farrell, N.; Kiley, D. M.; Schmidt, W.; Hacker, M. P. Chemical properties and antitumor activity of complexes of platinum containing substituted sulfoxides [PtCl(R′R″SO)(diamine)]-NO_3. Chirality and leaving group ability of sulfoxide affecting biological activity. *Inorg. Chem*. **1990**, *29*, 397–403.

(88) Fuks, L.; Samochocka, K.; Anulewicz-Ostrowska, R.; Kruszewski, M.; Priebe, W.; Lewandowski, W. Structure and biological activity of cationic [PtLCl(DMSO)]NO_3. DMSO complex containing a chelate diaminosugar: methyl-3,4-diamino-2,3,4,6-tetradeoxy-α-L-lyxopyranoside. *Eur. J. Med. Chem*. **2003**, *38*, 775–780.

(89) Fischer, S. J.; Benson, L. M.; Fauq, A.; Naylor, S. Cisplatin and dimethyl sulfoxide react to form an adducted compound with reduced cytotoxicity and neurotoxicity. *Neurotoxicology* **2008**, *29*, 444–452.

(90) Monsù-Scolaro, L.; Mazzaglia, A.; Romeo, A.; Plutino, M. R.; Castriciano, M.; Romeo, R. Geometrical configuration of monomethyl-platinum(II) complexes driven by the size of entering nitrogen ligands. *Inorg. Chim. Acta* **2002**, *330*, 189–196.

(91) Kerrison, S. J. J.; Sadler, P. L. Solvolysis of *cis*-[$Pt(NH_3)_2Cl_2$] in dimethylsulphoxide and reactions of glycine with [$PtCl_3(Me_2SO)$]$^-$ as probed by ^{195}Pt nuclear magnetic resonance shifts and ^{195}Pt−^{15}N coupling constants. *Chem. Commun*. **1977**, 861–863.

(92) Sundquist, V. I.; Ahmed, K. J.; Hollis, L. S.; Lippard, S. J. Solvolysis reactions of *cis* and *trans*-diamminedichloroplatinum-(II) in dimethyl sulfoxide. Structural characterization and DNA binding of *trans*-[$Pt(NH_3)_2(Me_2SO)Cl$]$^+$. *Inorg. Chem*. **1987**, *26*, 1524–1528.

(93) Pasut, G.; Veronese, F. M. Polymer−drug conjugation, recent achievments and general strategies. *Prog. Polym. Sci*. **2007**, *32*, 933–961.

(94) Pasut, G.; Sergi, M.; Veronese, F. M. Anti-cancer PEG-enzymes: 30 years old, but still a current approach. *Adv. Drug Delivery Rev*. **2008**, *60*, 69–78.

(95) Furin, A.; Guiotto, A.; Baccichetti, F.; Pasut, G.; Deuschel, C.; Bertani, R.; Veronese, F. M. Synthesis, characterization and preliminary cytotoxicity assays of poly(ethylene glycol)−malonato-Pt−DACH conjugates. *Eur. J. Med. Chem*. **2003**, *38*, 739–749.

(96) Dhar, S.; Liu, Z.; Thomale, J.; Dai, H.; Lippard, S. J. Targeted single-wall carbon nanotubes-mediated Pt(IV) prodrug delivery using folate as a homing device. *J. Am. Chem. Soc*. **2008**, *130*, 11467–11476.

(97) Ren, Y.; Zhang, H.; Huang, J. Synthesis and cytotoxic activity of platinum complex immobilized by branched polyethylene glycol. *Bioorg. Med. Chem. Lett*. **2005**, *15*, 4479–4483.

(98) Zhang, P.; Gao, W. Y.; Turner, S.; Ducatman, B. S. Gleevec (STI-571) inhibits lung cancer cell growth (A549) and potentiates the cisplatin effect in vitro. *Mol. Cancer* **2003**, *2*, 1–9.

(99) Gately, D. P.; Howell, S. B. Cellular accumulation of the anticancer agent cisplatin: a review. *Br. J. Cancer* **1993**, *67*, 1171–1176.

(100) Scanlon, K. J.; Kashani-Sabet, M.; Tone, T.; Funato, T. Cisplatin resistance in human cancers. *Pharmacol. Ther*. **1991**, *52*, 385–406.

(101) Marzano, C.; Gandin, V.; Folda, A.; Scutari, G.; Bindoli, A.; Rigobello, M. P. Inhibition of thioredoxin reductase by auranofin induces apoptosis in cisplatin-resistant human ovarian cancer cells. *Free Radical Biol. Med*. **2007**, *42*, 872–881.

(102) Zinkewich-Peotti, K.; Andrews, P. A. Loss of *cis*-diamminedichloroplatinum(II) resistance in human ovarian carcinoma cells selected for rhodamine 123 resistance. *Cancer Res*. **1992**, *52*, 1902–1906.

(103) Wersinger, C.; Rebel, G.; Lelong-Rebel, I. H. Detailed study of the different taurine uptake systems of colon Lo Vo MDR and non-MDR cell lines. *Amino Acids* **2000**, *19*, 667–685.

(104) Türk, D.; Szakács, G. Relevance of multidrug resistance in the age of targeted therapy. *Curr. Opin. Drug Discovery Dev*. **2009**, *12*, 246–252.

(105) Kamazawa, S.; Kigawa, J.; Kanamori, Y.; Itamochi, H.; Sato, S.; Iba, T.; Terakawa, N. Multidrug resistance gene-1 is a useful predictor of Paclitaxel-based chemotherapy for patients with ovarian cancer. *Gynecol. Oncol*. **2002**, *86*, 171–176.

(106) Siddik, Z. H. Cisplatin: mode of cytotoxic action and molecular basis of resistance. *Oncogene* **2003**, *22*, 7265–7279.

(107) Ormerod, M. G.; Orr, R. M.; Peacock, J. H. The role of apoptosis in cell killing by cisplatin a flow cytometric study. *Br. J. Cancer* **1994**, *69*, 93–100.

(108) Nicoletti, I.; Migliorati, G.; Pagliacci, M. C.; Grignani, F.; Riccardi, C. A rapid and simple method for measuring thymocyte apoptosis by propidium iodide staining and flow cytometry. *J. Immunol. Methods* **1991**, *139*, 271–279.

(109) Ormerod, M. G.; Collins, M. K. L.; Rodriguez-Tarduchy, G.; Robertson, D. Apoptosis in Interleukin-3 dependent haemopoietic cells: quantification by two flow cytometric methods. *J. Immunol. Methods* **1992**, *153*, 57–65.

(110) Perego, P.; Giarola, M.; Righetti, S. C.; Supino, R.; Caserini, C.; Delia, D.; Pierotti, M. A.; Miyashita, T.; Reed, J. C.; Zunino, F. Association between cisplatin resistance and mutation of p53 gene and reduced bax expression in ovarian carcinoma cell systems. *Cancer Res*. **1996**, *56*, 556–562.

(111) Komarov, P. G.; Komarova, E. A.; Kondratov, R. V.; Cristov-Tselkov, K.; Coon, J. S.; Chernov, M. V.; Gudkov, A. V. A chemical inhibitor of p53 that protects mice from the side effects of cancer therapy. *Science* **1999**, *285*, 1733–1737.

(112) Sedletska, Y.; Giraud-Panis, M. J.; Malinge, J. M. Cisplatin is a DNA-damaging antitumour compound triggering multifactorial biochemical responses in cancer cells: importance of apoptotic pathways. *Curr. Med. Chem. Anticancer Agents* **2005**, *5*, 251–65.

(113) Almeida, G. M.; Duarte, T. L.; Steward, W. P.; Jones, G. D. D. Detection of oxaliplatin-induced DNA crosslinks in vitro and in cancer patients using the alkaline comet assay. *DNA Repair* **2006**, *5*, 219–225.

(114) Heringova, P.; Woods, J.; Mackay, F. S.; Kasparkova, J.; Sadler, P. J.; Brabec, V. Transplatin is cytotoxic when photoactivated: enhanced formation of DNA cross-links. *J. Med. Chem*. **2006**, *49*, 7792–7798.

(115) Perrin, C. L.; Dwyer, T. J. Application of two-dimensional NMR to kinetics of chemical exchange. *Chem. Rev.* **1990**, *90*, 935–967.
(116) Venzo, A.; Bisello, A.; Ceccon, A.; Manoli, F.; Santi, S. Low hapticity intermediates in the carbonylation of (η^5-2,6-dimethyl-5-hydro-*s*-indacenide)-Ir(η^4-COD). *Inorg. Chem. Commun.* **2000**, *3*, 1–4.
(117) Bax, A.; Subramanian, S. Sensitivity-enhanced two dimensional heteronuclear shift correlation NMR spectroscopy. *J. Magn. Reson.* **1986**, *67*, 565–569.
(118) Drobny, G.; Pines, A.; Sinton, S.; Weitekamp, D. P.; Wemmer, D. Fourier transform multiple quantum nuclear magnetic resonance. *Faraday Symp. Chem. Soc.* **1978**, *13*, 49–55.
(119) Otting, G.; Wüthrich, K. Efficient purging scheme for proton-detected heteronuclear two-dimensional NMR. *J. Magn. Reson.* **1988**, *76*, 569–574.
(120) Bax, A.; Summers, M. F. ^{1}H and ^{13}C assignments from sensitivity-enhanced detection of heteronuclear multiple-bond connectivity by 2D multiple quantum NMR. *J. Am. Chem. Soc.* **1986**, *108*, 2093–2094.
(121) Fracarollo, D.; Bertani, R.; Mozzon, M.; Belluco, U.; Michelin, R. A. Synthesis and spectroscopic investigation of *cis* and *trans* isomers of bis(nitrile)dichloroplatinum(II) complexes. *Inorg. Chim. Acta* **1992**, *201*, 15–22.
(122) Kukushkin, V. Y.; Tkachuk, V. M. Synthesis, thermal isomerization in solution and in solid phase of the complexes [Pt(NCR)$_2$-Cl$_2$]. *Z. Anorg. Allg. Chem.* **1992**, *61*, 123–126.
(123) North, A. T. C.; Philips, D. C.; Mathews, F. S. A semi-empirical method of absorption connection. *Acta Crystallogr., Sect. A: Found. Crystallogr.* **1968**, *24*, 351–359.
(124) Altomare, A.; Burla, M. C.; Camalli, M.; Cascarano, G. L.; Giacovazzo, C.; Guagliardi, A.; Moliterni, A. G. G.; Polidori, G.; Spagna, R. Computer programs: SIR97: a tool for crystal structure determination and refinement. *J. Appl. Crystallogr.* **1999**, *32*, 115–119.
(125) Sheldrick, G. M. *SHELXL-97, Program for the Refinement of Crystal Structures*; University of Göttingen: Göttingen, 1997.
(126) Farrugia, L. J. WinGX suite for small molecule single-crystal crystallography. *J. Appl. Crystallogr.* **1999**, *32*, 837–838.
(127) Alley, M. C.; Scudiero, D. A.; Monks, A.; Hursey, M. L.; Czerwinski, M. J.; Fine, D. L.; Abbott, B. J.; Mayo, J. G.; Shoemaker, R. H.; Boyd, M. R. Feasibility of drug screening with panels of human tumor cell lines using a microculture tetrazolium assay. *Cancer Res.* **1988**, *48*, 589–601.
(128) Lowry, O. H.; Rosebrough, N. J.; Farr, A. L.; Randall, R. J. Protein measurement with the Folin phenol reagent. *J. Biol. Chem.* **1951**, *193*, 265–275.
(129) Woods, J. A.; Bilton, R. F.; Young, A. J. β-Carotene enhances hydrogen peroxide-induced DNA damage in human hepatocellular HepG2 Cells. *FEBS Lett.* **1999**, *449*, 255–258.